

Review

Wearable epidermal sensors with surface-enhanced Raman spectroscopy for personalized health

Yuanchao Liu (刘元超)¹, Binbin Zhou (周彬斌)⁸, Xiujuan Hu (胡秀娟)³, Yunchen Long (龙耘辰)¹⁰, Shaofei Li (李绍飞)⁷, Chaochao Sun (孙超超)¹, Annan Chen (陈安南)¹, Xiu Liang (梁秀)^{3,7,10}, Yu Song (宋宇)⁴, Dangyuan Lei (雷党愿)^{3,7,10}, Tailin Xu (许太林)⁹, Lianbo Guo (郭连波)⁶, Condon Lau (刘康德)^{3,*}, Wei Luo (罗为)⁵, and Chwee Teck Lim (林水德)²

¹Department of Mechanical Engineering, City University of Hong Kong, Kowloon, Hong Kong SAR 999077, China

²Department of Biomedical Engineering, National University of Singapore, Singapore 117583, Singapore

³Department of Physics, City University of Hong Kong, Kowloon, Hong Kong SAR 999077, China

⁴Department of Biomedical Engineering, City University of Hong Kong, Kowloon, Hong Kong SAR 999077, China

⁵School of Integrated Circuits, Huazhong University of Science and Technology, Wuhan 430074, China

⁶Wuhan National Laboratory for Optoelectronics (WNLO), Huazhong University of Science and Technology, Wuhan 430074, China

⁷Hong Kong Branch of National Precious Metals Material Engineering Research Centre, City University of Hong Kong, 83 Tat Chee Avenue, Kowloon, Hong Kong SAR 999077, China

⁸Shenzhen Institute of Advanced Electronic Materials, Shenzhen Institute of Advanced Technology, Chinese Academy of Sciences, Shenzhen 518055, China

⁹The Institute for Advanced Study (IAS), Shenzhen University, Shenzhen, Guangdong 518060, China

¹⁰Department of Materials Science and Engineering, City University of Hong Kong, Kowloon, Hong Kong SAR 999077, China

*Correspondence: condon.lau@cityu.edu.hk

<https://doi.org/10.1016/j.device.2025.100939>

THE BIGGER PICTURE Wearable sensors can deliver real-time and noninvasive monitoring of health biomarkers from biofluids such as sweat, interstitial fluid, and wound exudate. Surface-enhanced Raman spectroscopy (SERS) is one such method for detecting molecular biomarkers with high sensitivity and specificity. However, practical integration of SERS into flexible and wearable devices faces challenges, including substrate design, plasmonic material stability, and signal reproducibility. This review summarizes recent progress in flexible substrate (e.g., textile or hydrogel) design, plasmonic nanomaterial (e.g., gold or silver nanoparticles) optimization, and biofluid sampling strategies and highlights challenges hindering clinical translation. Future directions are outlined to improve device reliability, user comfort, and applicability in real-world healthcare.

SUMMARY

Wearable epidermal sensors can realize real-time, minimally invasive or noninvasive monitoring of biomarkers such as those found in sweat, interstitial fluid (ISF), and wound exudate. Conventional electrochemical and colorimetric sensing techniques face challenges in achieving reliable multiplexed detection. Surface-enhanced Raman spectroscopy (SERS) can offer molecular specificity for detecting trace biomarkers. This review examines the use of SERS in epidermal sensors, with a focus on material design, substrate functionalization, and biofluid sampling strategies. We discuss opportunities for future development in device structural design, the use of plasmonic materials, multi-functional integration, and AI-driven diagnostics.

INTRODUCTION

Wearable epidermal sensors can enable multiplexed detection of biomarkers in biofluids,¹ such as sweat,^{2–4} interstitial fluid (ISF),^{5,6} and wound exudate,^{7,8} where the biomarkers are converted into optical or electronic signals for health assessment (Figure 1A).⁹ Among biofluids, sweat is widely studied due to its ease of collection and multiple chemical information. Wearable epidermal sensors with microfluidic channels are used to collect sweat directly from the skin (Figure 1B).^{10,14} ISF has at-

tracted attention for its similarity to plasma, making it a valuable source of biomarkers. Notably, as shown in Figure 1C, ISF is extracted through microneedle arrays, offering less invasive monitoring compared to traditional blood sampling.^{6,15,16} Meanwhile, monitoring wound exudate (Figure 1D) can continuously assess the wound environment, tracking factors such as pH, enzyme activity, and infection biomarkers.^{11,17}

While current sensing strategies, such as electrochemical (Figure 1E) and colorimetric (Figure 1F) methods, have been widely adopted in wearable sensors due to their simplicity and

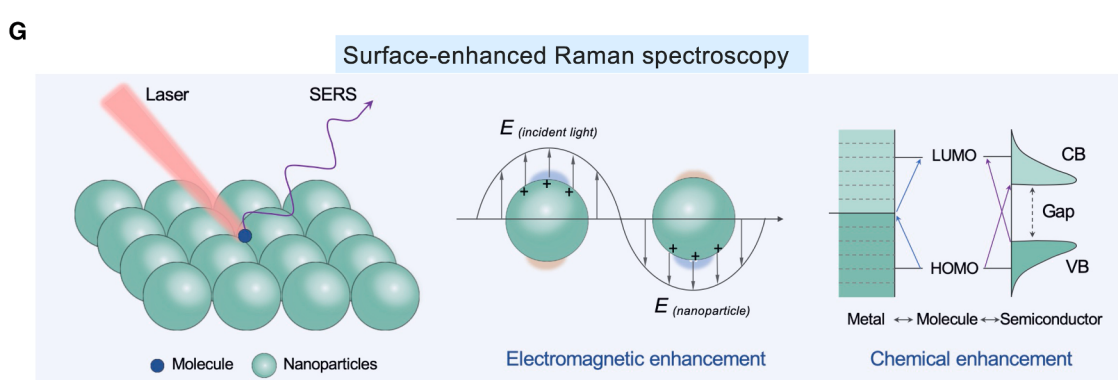
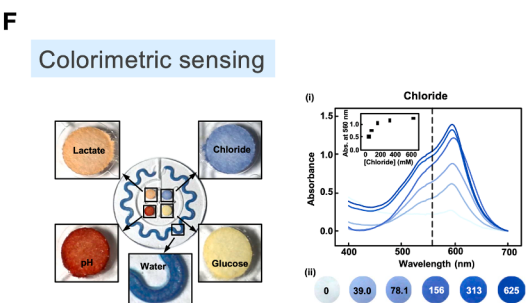
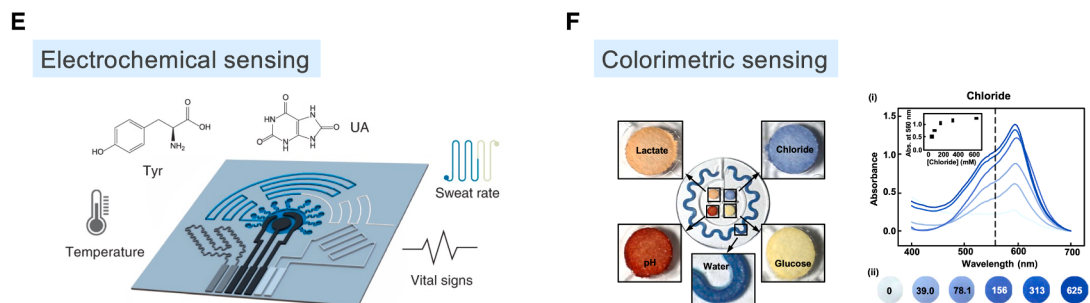
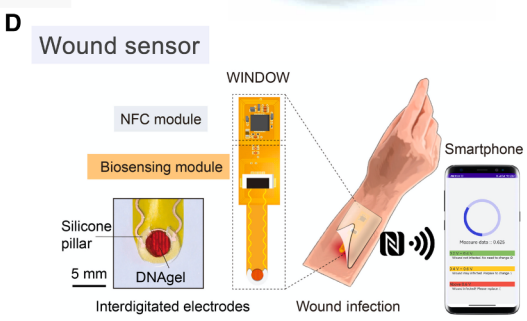
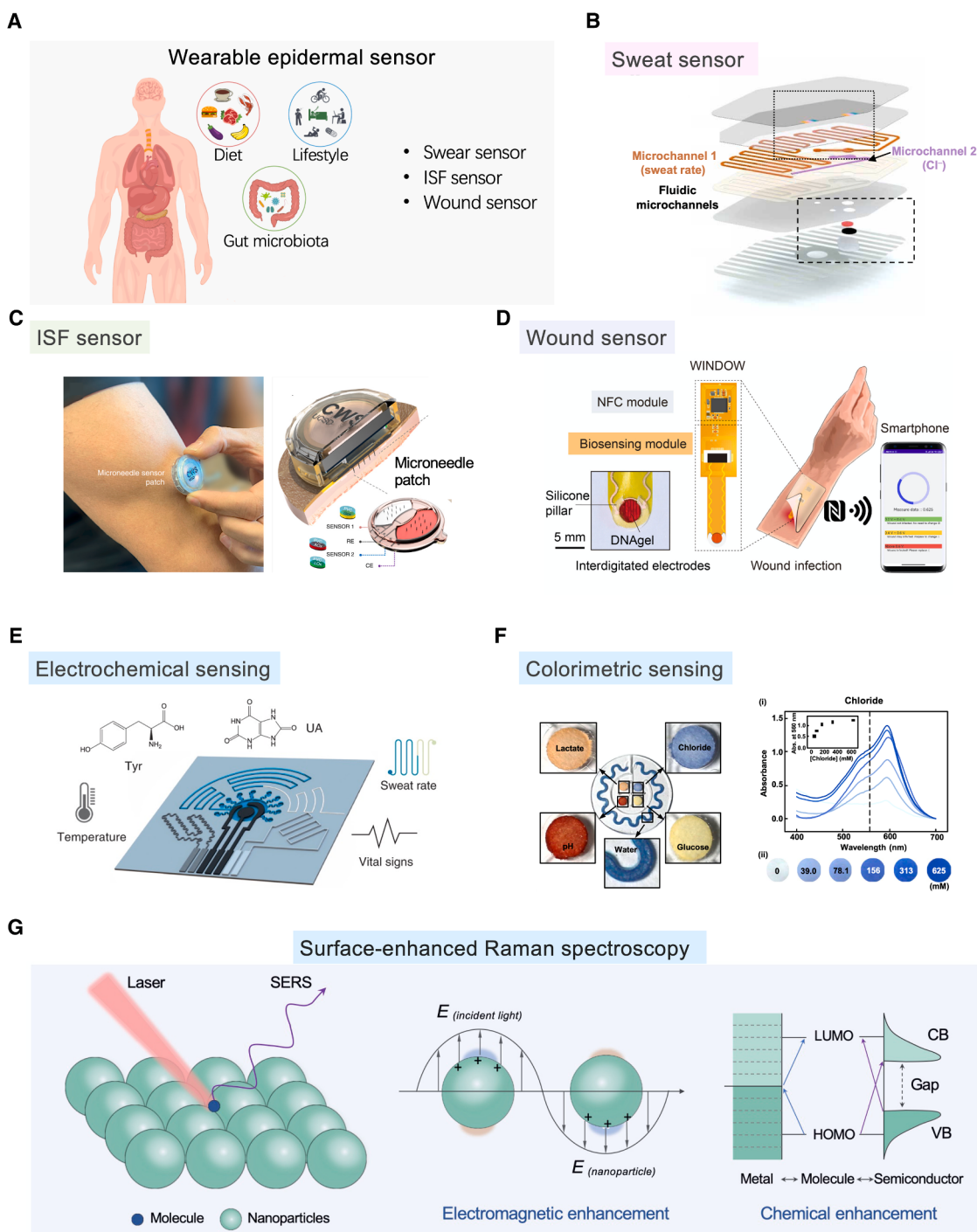


Figure 1. Overview of wearable epidermal sensors

(A) Schematic showing the three epidermal sensors.⁹ Copyright 2022, the author(s), under exclusive license to Springer Nature.

(B) Representative work of sweat sensor.¹⁰ Reproduced under terms of the CC-BY license.

(C) Representative work of ISF sensor.⁶ Copyright 2022, Springer Nature.

(D) Representative work of wound exudate sensor.¹¹ Copyright 2021, the American Association for the Advancement of Science.

(E) Electrochemical sensing strategy.¹² Copyright 2019, Springer Nature.

(F) Colorimetric sensing strategy.¹³ Copyright 2016, the American Association for the Advancement of Science.

(G) Schematic of SERS principle and SERS signal enhancement mechanism.

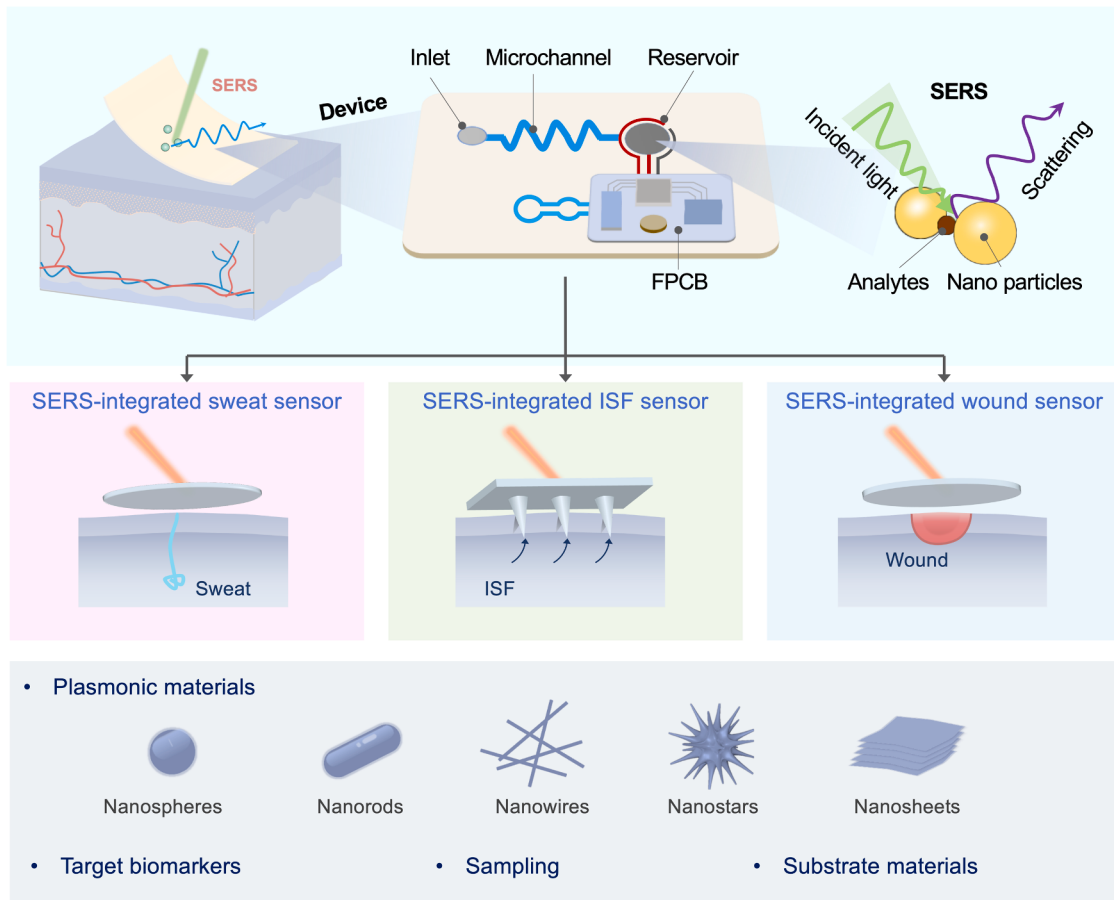


Figure 2. Schematic of SERS-integrated wearable epidermal sensors

Three types of epidermal sensors (sweat sensor, ISF sensor, and wound exudate sensor) are discussed from different perspectives.

relatively high sensitivity, challenges remain in achieving reliable detection in complex biological environments.^{12,13} Specifically, electrochemical sensors are prone to interference from ionic changes and pH fluctuations, which affect signal accuracy and stability. Colorimetric methods lack the ability to detect multiple analytes simultaneously, especially in complex or low-concentration samples. These inherent limitations restrict their use in real-time, multiplexed biochemical sensing.^{18,19} In contrast, surface-enhanced Raman spectroscopy (SERS) (Figure 1G) enables detection of biomarkers based on their "fingerprints," showing great potential for detecting trace analytes with high specificity.

SERS can amplify Raman scattering signals by several orders of magnitude, enabling the detection of ultra-trace-level concentrations of biomarkers. In addition, SERS provides specific diagnostic information by identifying analytes through their unique molecular fingerprints, and its compatibility with various flexible substrates makes it suitable for use in wearable sensors.²⁰ However, the practical applications of SERS still face challenges, including the lack of reproducible substrates, rapid sampling, and efficient signal processing.²¹

This review will discuss the use of SERS in wearable epidermal sensors (Figure 2). The fundamental principles

of SERS are introduced, followed by its use in detecting specific types of biofluids, i.e., sweat, ISF, and wound exudate. We will discuss the selection of plasmonic materials, substrate materials, and sampling methods. We will share our perspectives on the future of SERS in wearable devices, outlining its potential challenges and proposing future research directions.

OPERATING PRINCIPLE OF SERS

Raman spectroscopy can acquire detailed molecular information through light scattering, revealing properties such as chemical structure, polymorphism, and crystallinity.²² However, traditional Raman spectroscopy suffers from certain limitations, including low signal intensity and poor sensitivity.²² Compared to conventional Raman scattering, which produces weak signals due to inelastic photon scattering by molecular vibrations, SERS amplifies these signals when molecules are near nanostructured surfaces such as gold or silver. This enhancement arises from the interaction between incident light and conduction electrons, leading to intense local electromagnetic (EM) fields known as localized surface plasmon resonance (LSPR).²³ In a typical SERS process, analyte molecules adsorbed onto metallic nanostructures

experience amplified excitation and scattered fields. This dual enhancement increases the Raman scattering cross-section by several orders of magnitude, enabling trace-level detection. SERS preserves the fundamental vibrational specificity of Raman transitions while boosting signal intensity via nanostructure-mediated EM field effects.^{24,25}

Although the precise mechanisms of SERS are still under active investigation, two main theories are recognized (Figure 1G).^{25–27} One of these theories is that the EM enhancement originates from the intense and highly localized EM fields generated at “hotspots,” which are found at nanogaps or sharp features of plasmonic nanostructures. Molecules located within these regions experience simultaneous amplification of both the excitation and scattered Raman fields, resulting in signal enhancements ranging from 10^4 to 10^8 and up to 10^{10} in optimized substrates.^{27–29} The second theory is the chemical enhancement mechanism (CM), although it contributes less than EM effects, where the analyte molecules form strong chemisorption bonds with the metal surface. It involves charge transfer between molecular orbitals and the metal’s Fermi level, modulating molecular polarizability and enhancing the Raman signal by one to two orders of magnitude. The magnitude of chemical enhancement depends on factors such as adsorption geometry, bonding strength, and electronic structure alignment at the molecule-metal interface.²⁷ Despite sustained research into these mechanisms, it is well established that SERS can produce several orders of magnitude in signal enhancement, such as for the detection of biomolecules.^{25,26}

SERS has been applied in various domains, such as nanomaterial synthesis, chemical reaction monitoring, and biomedical diagnostics.^{22,30,31} It has also been integrated into wearable sensors for enabling real-time,^{32,33} minimally invasive or noninvasive molecular analysis of biological fluids, including sweat, ISF, and wound exudate.^{33–36}

SERS is particularly beneficial for wearable sensing due to its high molecular specificity and sensitivity, which are essential for detecting trace biomarkers in complex biological matrices.³⁷ Meanwhile, the use of plasmonic nanostructures, fabricated on flexible substrates, amplifies weak Raman signals that are difficult to detect by conventional sensors.^{18,38} In addition, SERS offers a label-free detection approach, which eliminates the need for chemical modifications or additional reagents, thereby simplifying sensor design and operation.³⁹ Furthermore, the ability of SERS to acquire signals quickly and facilitate multiplexed detection makes it highly suitable for real-time health monitoring in wearable devices.³⁷

SERS FOR SWEAT ANALYSIS

Sweat is rich in diverse biomarkers that indicate human physiological health, and SERS-integrated sensors can be used for analyzing biomarkers found in sweat, such as metabolites, proteins, hormones, and drugs.^{18,19} The performance of these sensors can be enhanced by the design and selection of substrate materials and sweat acquisition methods. In this section, we discuss the literature and challenges associated with SERS-integrated sweat sensors for sweat analysis (Figure 3A), including sampling strategies and plasmonic materials.

Sweat sampling methods

Effective sweat sampling methods are essential for high-quality SERS detection, as factors such as sweat volume, collection efficiency, and purity directly influence the strength and accuracy of the signal. Typical sweat acquisition techniques include direct contact, polydimethylsiloxane (PDMS)-based microfluidic collection, and paper-based microfluidic collection (Figure 3B).^{40,43,44} Among them, the direct contact method relies on the close interaction between the wearable device and skin, enabling rapid detection of sweat components with minimal volumes by integrating signal-enhancing materials with the sweat.^{44–46} This method does not depend on fluid flow, which helps ensure collection efficiency and accuracy under low sweat conditions and also minimizes external contamination, ensuring the purity and sensitivity of the signal (Figure 3D).³⁵

Flexible microfluidic designs can help improve both sweat collection efficiency and sensor stability. For example, PDMS-based microfluidic channels offer flexibility and stretchability for high-throughput or continuous sweat collection.^{40,47,48} By utilizing the synergistic effects of natural sweat gland secretion pressure and capillary forces, skin-interface microfluidic patches can collect sweat while reducing evaporation and contamination.^{49,50} Zhang et al.⁴⁰ developed a PDMS-based platform integrated with plasmonic metasurfaces featuring homogeneous mushroom-shaped hotspots, enabling fast SERS detection of pH, lactate, and urea in sweat (Figure 3E). Low-cost paper-based microfluidic collection methods can also be used to provide a simple yet effective solution for sweat collection.^{41,43} Mogera et al.⁴¹ designed plasmonic microfluidic channels with continuous pathways for real-time monitoring of sweat flow rate, sweat loss, and metabolites (Figure 3F). Han et al.⁴² developed a Janus textile-based collection system (Figure 3G), using superhydrophobic and superhydrophilic regions for unidirectional flow and efficient sweat collection, combined with an optical fiber to enhance SERS signal detection.

Plasmonic material selection and substrate design

SERS substrate material is essential to determine the sensitivity, stability, and durability of sensors. For sweat analysis, SERS substrates require strong Raman signal enhancement alongside flexibility and biocompatibility. Recent research has reported various nanomaterials in sweat analysis, including precious metals^{51–54} and oxide semiconductors.^{55,56} Furthermore, a well-designed structure can provide more hotspots to enhance Raman signals, such as those involving nanorods, nanostars, nanowires (NWs), and nanosheets (Figure 3C).^{49,57–59} SERS substrates with composite structures have been developed, providing more SERS enhancement hotspots through the synergistic effects of multiple structures.^{50,55,56}

For example, Zhu et al.⁵⁴ developed a wearable sensor using an omnidirectional plasmonic nanovoid array (OPNA), which is prepared by assembling a monolayer of metal nanoparticles (NPs) into the artificial plasmonic compound eye (APC). This composite structure renders a broadband and omnidirectional enhancement of hotspots in the delicate NP array while also maintaining the integrity of the hotspots against external mechanical deformations.

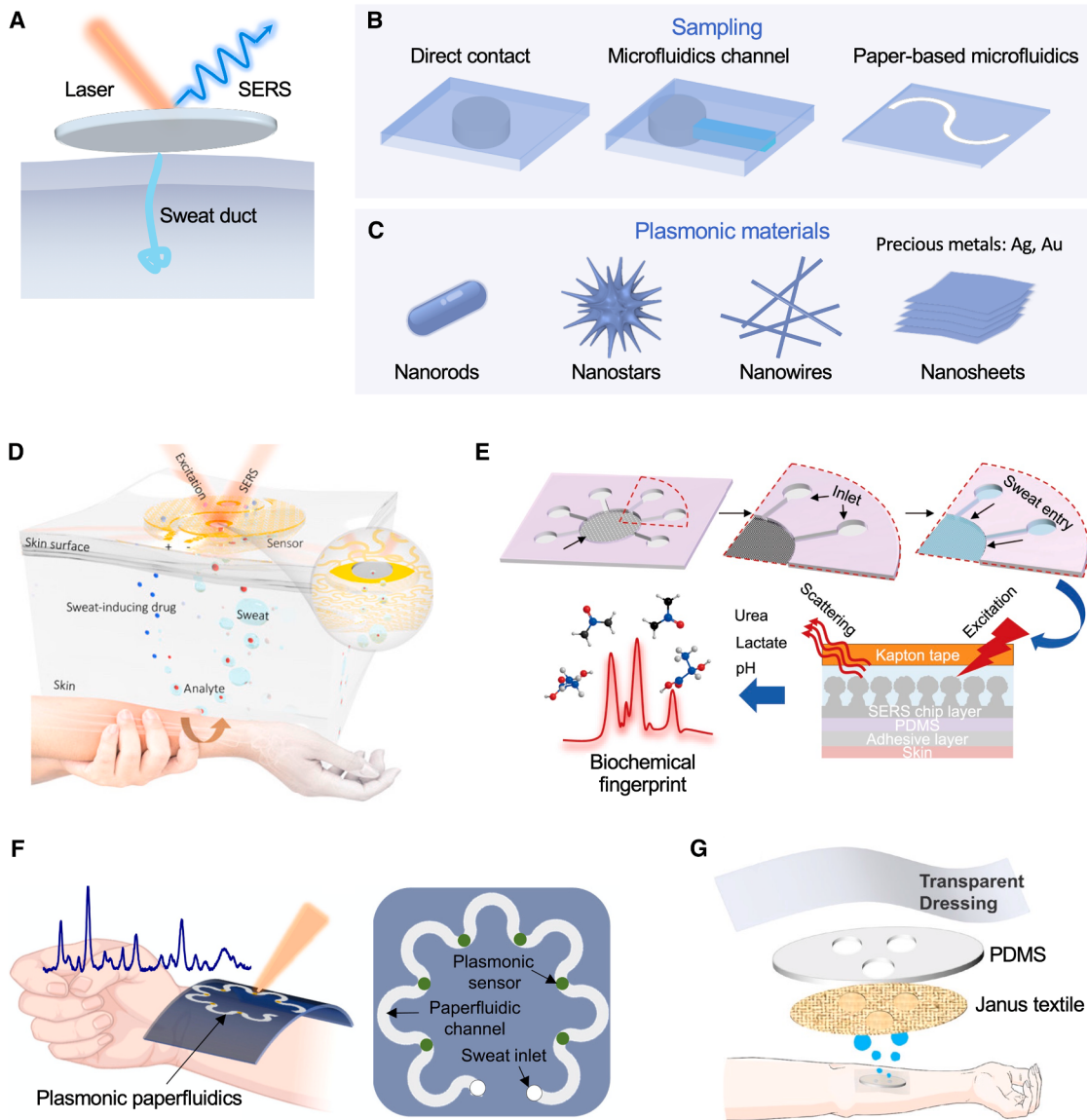


Figure 3. Characterization of SERS-integrated sweat sensor

- (A) Schematic showing SERS sensing sweat.
- (B) Schematic of sweat sampling methods.
- (C) Schematic showing plasmonic nanomaterials for SERS-integrated sweat sensor.
- (D) Representative work of direct contact sampling.³⁵ Copyright 2021, the American Association for the Advancement of Science.
- (E) Representative work of microfluidic channel sampling.⁴⁰ Reproduced under terms of the CC-BY license.
- (F) Representative work of paper-based microfluidics sampling.⁴¹ Reproduced under terms of the CC-BY license.
- (G) Sweat sampling method based on Janus textile.⁴² Copyright 2023, American Chemical Society.

In addition to precious metals and metal oxide semiconductors, advanced alternative materials have been investigated, including 2D materials such as 2D carbon nanomaterials, as well as metasurfaces and liquid metals.^{35,47,58,60,61} For instance, Yuan et al.⁴⁷ developed a wearable microfluidic chip featuring erasable liquid-metal plasmonic hotspots for glucose analysis (1 ng/L) in sweat.

Flexible materials, such as PDMS, paper, hydrogel-based, and textile-based materials, have been explored for creating

wearable devices.^{41,43,48} To obtain the optimal performance of SERS sensor substrates, it is important to combine platform materials with signal-enhancing materials. Deposition techniques are commonly used to achieve this combination.^{62,63} For instance, Rao et al.⁶⁴ developed a SERS substrate with a 3D network of Ag-deposited polyvinyl alcohol (PVA) nanofibers for detecting sweat and urine. Similarly, Liu et al.⁴⁴ used thermal evaporation to deposit Au onto PVA nanomeshes, resulting in a thin, flexible, stretchable, adhesive, and biocompatible Au

nanonet. This flexible and scalable substrate ensures good scalability for SERS sensors with its simple fabrication method. Although the integration of flexible substrates with plasmonic materials has shown promising results, several technical limitations persist. For instance, the adhesion between the enhancement layer and the substrate may degrade under repeated deformation or exposure to sweat. Moreover, conventional deposition methods often struggle to achieve uniform coverage on large areas or non-flat surfaces.

In conclusion, the integration of microfluidic systems and substrate design is important for efficient sweat capture, especially with considerations for signal generation and transmission in varying physiological conditions. The design of nanomaterials can help maintain the flexibility and mechanical stability of sensors. However, the variability of sweat secretion across individuals and its sensitivity to external factors (e.g., temperature, hydration, and physical activity) pose challenges to obtaining stable and reproducible SERS signals. Moreover, extended wear and continuous exposure to sweat can cause biofouling or degradation of the sensing interface, reducing detection accuracy and long-term device stability. Future research requires continuous optimization of material selection and design, further simplification of sweat collection systems, and advanced automation of signal processing to achieve widespread use of SERS-integrated sweat sensors in clinical and daily health monitoring.

SERS FOR ISF ANALYSIS

ISF is an extracellular fluid that facilitates the transport of nutrients, waste products, and signaling molecules. ISF is rich in biomarkers such as glucose, lactate, and proteins, which reflect the metabolic state of local tissues and the overall physiological health of the human body, making it highly valuable for diagnostic applications.^{65,66} SERS sensors can realize minimally invasive or noninvasive analysis of ISF, and their performance relies on optimizing sensor materials and acquisition methods (Figure 4A).^{72–74} In this section, we summarize the literature and challenges in wearable epidermal SERS sensors for ISF analysis.

ISF sampling using microneedles

Currently, ISF collection primarily relies on the use of microneedles, whose fabrication methods can be divided into three main types, i.e., molding, additive manufacturing, and subtractive manufacturing (Figure 4B).^{66,75} These methods differ in process characteristics and material compatibility, which impact the clinical applications of microneedles. Of the three, molding (also known as template based) is the most well-established microneedle fabrication technique, with a mold-filling-curing-forming process.^{76–78} Typically, polymer solutions or molten materials are injected into pre-formed silicone or metal molds, obtaining uniform material distribution through centrifugal or vacuum-assisted techniques. After physical or chemical curing, the microneedle array is obtained by demolding.^{32,67,68,74,79–82} This method exhibits advantages such as high process repeatability and cost effectiveness.⁷⁷ In comparison, additive manufacturing is not limited by some of the geometric con-

straints of traditional molds through layer-by-layer construction techniques, such as photopolymerization and fused deposition.^{83–86} For example, the stereolithography technique can fabricate complex microneedle configurations, including hollow structures and multi-level tapers.^{68,77,87} However, this method still faces some challenges, resulting from poor biocompatibility and low mechanical properties of photopolymer materials.⁷⁷ Finally, subtractive manufacturing employs selectively carving or micro-milling technology to machine metal billets.^{75,88,89} Although this method can provide high-precision microstructural fabrication, its high specialization of equipment and low processing efficiency limit large-scale clinical applications.^{6,77}

Besides the process characteristics, these three manufacturing techniques exhibit distinct material compatibility properties. In detail, molding is suitable for injection-molding polymer materials, additive manufacturing is constrained by the rheological properties of photopolymer materials, and subtractive manufacturing requires materials with sufficient machinability.⁷⁷ Therefore, the selection of the process should comprehensively consider material properties, microneedle functionality, and production economics.

Efficient collection of ISF is critical for achieving precise SERS detection. As minimally invasive collection devices, microneedle arrays have become ideal tools for ISF collection due to their minimal pain and high collection efficiency. Common ISF collection methods include swelling absorption of ISF and passive (i.e., via the capillary effect) or active collection based on hollow channels (Figure 4C). A common approach for ISF collection is utilizing hydrogel microneedles with water-absorbing swelling properties, which are typically fabricated through the molding method.⁹⁰ Upon penetrating the skin, they rapidly absorb ISF and swell, enhancing ISF extraction and demonstrating high efficiency in capturing target molecules (Figure 4D).^{67,91} However, the process of extracting ISF from hydrogel and releasing biomarkers for detection is often complicated and costly. For example, an additional procedure is required to extract ISF and metabolites from hydrogel microneedle (MN) using centrifugation (e.g., 10 k rpm for 5 min).⁹² Furthermore, the microliter-scale ISF extractions are diluted by diluents, limiting the detection to low-concentration biomarkers in ISF.^{93,94}

Designing microneedles with hollow channels is another approach for ISF collection (Figure 4E).^{32,68} Typically, hollow microneedles are fabricated through photopolymerization. After penetrating the skin, ISF is drawn into the hollow channels through capillary action.⁶⁶ To improve ISF collection efficiency, external excitation sources (e.g., suction cups and vacuum tubes) are used to actively collect larger ISF volumes.^{32,95,96} Some studies have combined porous microneedles with microfluidic technology to enhance collection efficiency and enable continuous monitoring. For example, by integrating porous microneedles with microfluidic chips, sufficient amounts of ISF have been collected through capillary action or negative pressure extraction.^{80,97} Therefore, the collection and analysis processes are integrated to reduce traditional sample processing steps. Zhang et al.³² developed a microfluidic-based hollow microneedle device that utilized negative pressure generated by finger pressure, achieving efficient ISF collection and minimally invasive uric acid monitoring (Figure 4F).

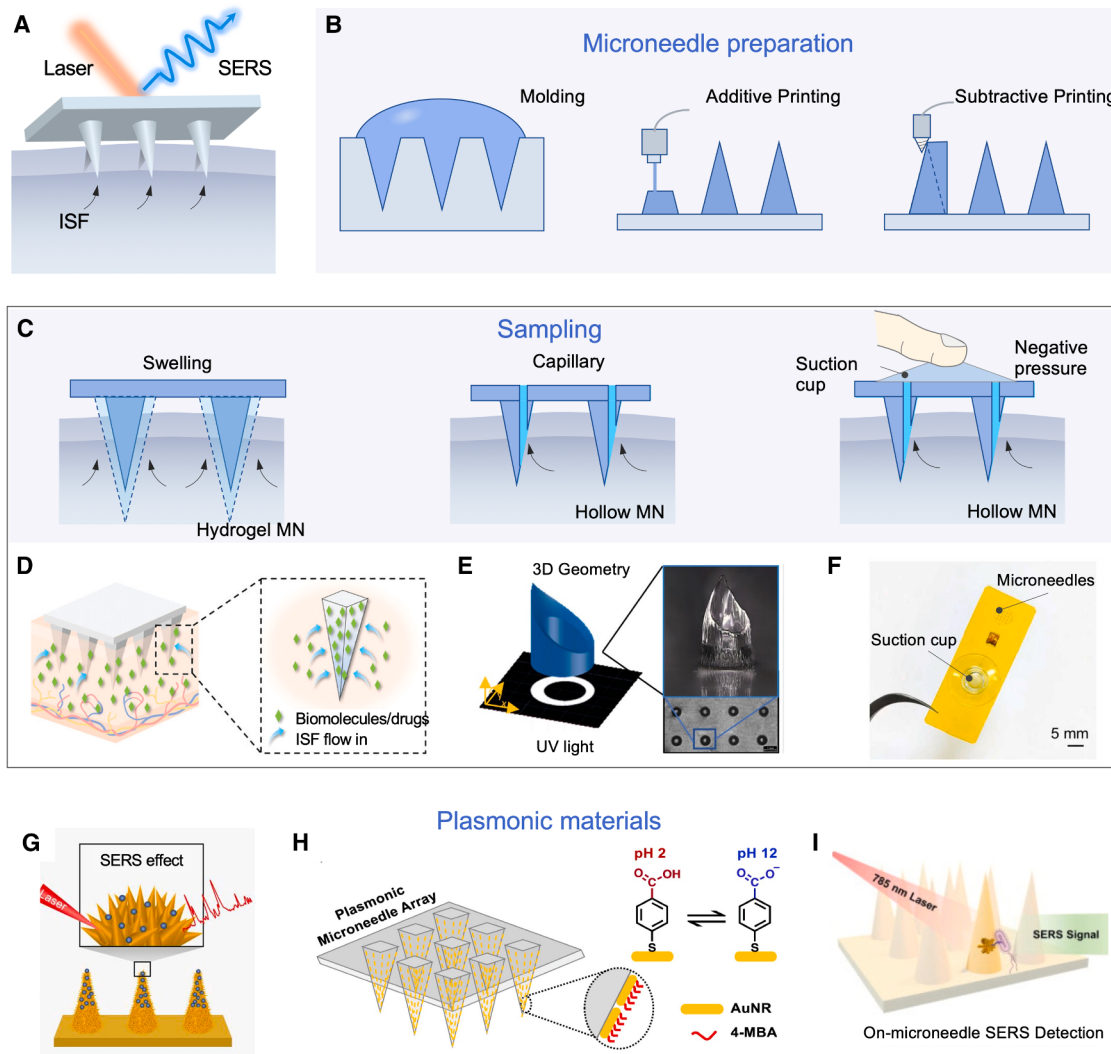


Figure 4. Characterization of SERS-integrated ISF sensor

- (A) Schematic showing SERS sensing ISF.
- (B) Schematic showing microneedle preparation methods for SERS-integrated ISF sensor.
- (C) Schematic of ISF sampling methods.
- (D) Representative work of swelling sampling.⁶⁷ Copyright 2023, Wiley-VCH.
- (E) Representative work of capillary sampling.⁶⁸ Reproduced under terms of the CC-BY license.
- (F) Representative work of suction cup sampling.³² Copyright 2023, Elsevier B.V.
- (G) Schematic showing microneedles with Au nanoflowers for SERS signal enhancement.⁶⁹ Reproduced under terms of the CC-BY license.
- (H) Schematic of microneedles, covered by functionalized Au nanorods with pH-sensitive molecules.⁷⁰ Reproduced under terms of the CC-BY license.
- (I) Schematic showing microneedles, functionalized with specific aptamers for rapid detection of specific bacteria.⁷¹ Copyright 2022, Elsevier B.V.

Different types of SERS-integrated microneedle sensors pose varying levels of skin injury and infection risk during practical applications. Hydrogel microneedles, which swell after insertion and remain in prolonged contact with the skin, increase the likelihood of localized irritation and microbial colonization under humid conditions. Hollow microneedles feature open channels that provide direct pathways for microbial invasion and are often associated with reduced user comfort due to their larger dimensions. Besides, rigid microneedles may offer superior mechanical strength and structural stability, but their limited flexibility leads

to greater mechanical damage to skin tissue. Future designs should balance sampling efficiency, biocompatibility, and user comfort when selecting appropriate microneedle structures.

Plasmonic material selection and substrate design

In SERS-based ISF detection, the selection of plasmonic materials (e.g., precious metal nanostructures) and the design of the substrate are important.^{69,98} For example, Au nanoflowers, Au nanorods, and Au nanodisks can be combined with biocompatible polymers (e.g., PLGA, PEGDA, and GelMA)

to form microneedle arrays, where the polymers serve as the mechanical backbone of the microneedle tips, providing structural support and transdermal capability, while the AuNPs act as a surface coating to improve biocompatibility and transdermal sensing efficiency.^{69,71}

With a branched structure, gold nanoflowers could form more hotspots to enhance the intensity of SERS signals, and they have been used to detect trace methylene blue (with a limit of detection [LOD] of 50 nM) and other biomarkers (Figure 4G).⁶⁹ In addition to detecting common biomarkers, gold nanorods functionalized with pH-sensitive molecules (e.g., 4-mercaptopbenzoic acid) have been reported for the quantification of pH values within a certain range (5–9) (Figure 4H).⁷⁰ By functionalizing microneedle surfaces with specific aptamers and multi-functional coatings, the binding ability of the microneedles to target molecules is enhanced, enabling the detection of specific bacteria (e.g., *Escherichia coli*) (Figure 4I).⁷¹ In addition, composite nanostructures have emerged as a research focus. For example, core-satellite AuNPs can be assembled on microneedle surfaces, enabling sensitive monitoring of drug release.⁹⁰

Future research is required to address several challenges. The limited ISF volume obtained via microneedles may reduce analyte availability for SERS detection, affecting signal intensity and sensitivity. Moreover, prolonged microneedle use may alter local tissue conditions, potentially compromising signal reproducibility. The selection and design of materials should be optimized to improve their biocompatibility and mechanical stability. For example, control over the size, shape, and interparticle spacing of plasmonic nanostructures is essential for tuning LSPR and maximizing hotspot density to maximize the enhancement of SERS signals.^{24,25} Balancing the mechanical flexibility and sampling efficiency of collection devices remains a critical design challenge. While enhanced flexibility contributes to improved user comfort, it compromises microneedle insertion efficiency and structural integrity. To address this trade-off, future efforts should focus on advanced structural engineering, such as the integration of rigid, microneedle tips with compliant, flexible substrates. Moreover, signal processing methods should be enhanced with higher intelligence and automation to improve detection accuracy and simplify operation.

SERS FOR WOUND MONITORING

Wound exudate is a biofluid involved in the healing process, comprising water, electrolytes, proteins, inflammatory cells, bacteria, and diverse biomarkers (Figure 5A). It originates from plasma exudation, inflammatory secretions, and ISF. Over time, the volume and composition of exudate evolve dynamically, reflecting the wound's healing status, and its biomarkers can provide insights into the healing progression and inform therapeutic strategies.¹⁰²

Wound exudate sampling methods

Raman spectroscopy under low laser power (e.g., <10 mW) and near-infrared excitation (e.g., 785 nm) enables noninvasive direct analysis (Figure 5B). By modulating the laser power, this technique avoids tissue damage while maintaining sufficient signal acquisition, which is valuable for chronic wound manage-

ment.¹⁰³ It allows for continuous monitoring for signs of infection or inflammation. However, the inherently weak Raman signals and susceptibility to interference limit the sensitivity and accuracy of direct detection.

To enhance signal intensity, SERS-active plasmonic patches are introduced (Figure 5B). These substrates amplify Raman signals upon contact with the wound surface, enabling precise detection of target molecules or pathogens in exudate (Figure 5D).^{99,104} For example, SERS probes loaded on chitosan membranes have been applied to acute wounds, with the probes facing the wound to acquire *in vivo* SERS spectra that reflect the redox status during healing.¹⁰⁴

Additional tools have been developed to extract wound exudate for subsequent SERS analysis (Figure 5B). For example, a swab-based sampling method (Figure 5E) used cotton swabs to collect exudate from wounds, which was then transferred to AgNP solutions for SERS analysis.¹⁰⁰ This method is advantageous for deep or inaccessible wounds, enabling sample-to-data workflows, reducing interference from complex SERS substrate components on wound healing.

Plasmonic material selection and substrate design

In SERS-based wound detection, precious metal nanoparticles (e.g., AuNPs and AgNPs) are popular materials due to their EM enhancement effects.^{105,106} To improve performance and biocompatibility, researchers have explored materials such as core-shell nanostructures and composites.^{105,107,108} For instance, Au-Ag core-shell NPs were used to monitor peroxynitrite (ONOO⁻) fluctuations in diabetic wound models (Figure 5C).¹⁰² Similarly, AuNPs immobilized on Cu²⁺-C₃N₄ nanosheets have been integrated into SERS-active nanozymes, enabling real-time tracking of H₂O₂ dynamics during wound healing.¹⁰⁹

Apart from the enhancement effect, substrate materials require flexibility, breathability, and biocompatibility for long-term wearability. Both polymer-based and cellulose fiber matrices have been reported.^{104,106} For example, a cellulose-fiber-based plasmonic membrane has shown potential for point-of-care detection of biomarkers, like tumor necrosis factor- α (TNF- α) and matrix metalloproteinase-9 (MMP-9) in chronic wound exudate.¹⁰⁴

Wound exudate contains kinds of biomarkers such as glucose, lactate, cytokines, proteins, and pathogens (e.g., bacteria and fungi).¹⁸ SERS-integrated sensors are developed to target these analytes, providing diagnosis of infections.^{102,110,111} For instance, SERS detection of ONOO⁻ in diabetic wounds achieved dynamic monitoring of the inflammation and therapeutic responses.¹⁰² Besides, Guo et al.¹¹¹ developed Ag@Prussian blue core-satellite nanoprobes for near-zero-background detection of residual bacteria during healing. SERS sensors have also been integrated into closed-loop diagnostic-therapeutic systems (Figures 5F),^{101,109,111} providing real-time feedback to adjust treatment strategies. For example, He et al.¹⁰¹ developed a DTTC-conjugated Au-Ag nanoshell system for SERS imaging and photothermal eradication of multidrug-resistant bacteria (Figure 5G). This system not only achieved noninvasive, high-sensitivity detection (down to 300 CFU/mL for methicillin-resistant *Staphylococcus aureus*), and real-time bacterial monitoring for up to 8 days but also eradicated Gram-positive

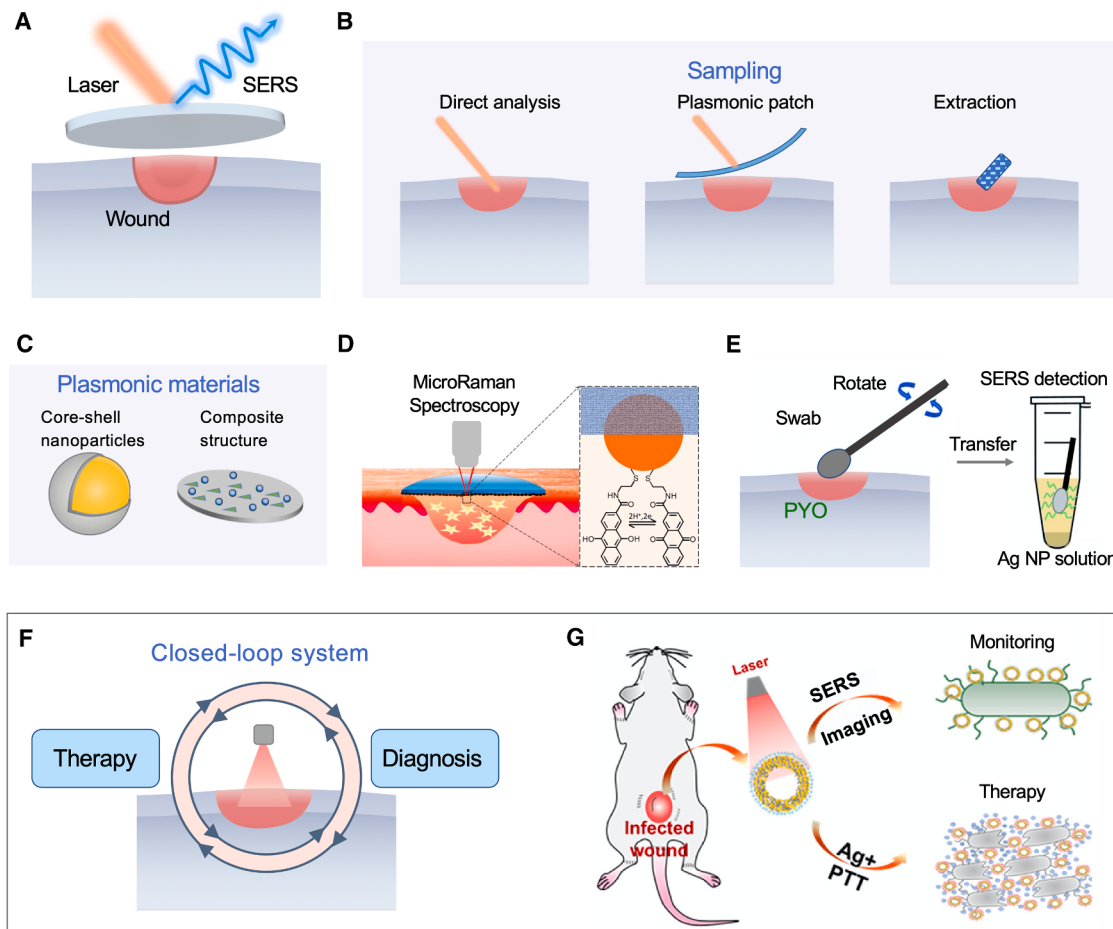


Figure 5. Characterization of SERS-integrated wound sensor

- (A) Schematic showing SERS sensing wound exudate.
(B) Schematic of wound exudate sampling methods.
(C) Schematic of plasmonic materials.
(D) Representative work of direct analysis.⁹⁹ Copyright 2018, American Chemical Society.
(E) Representative work of extraction sampling using swab.¹⁰⁰ Reproduced with permission. Copyright 2021, Royal Society of Chemistry.
(F) Schematic showing closed-loop system with therapy and diagnostics.
(G) Representative work of closed-loop system.¹⁰¹ Copyright 2020, Elsevier.

E. coli, Gram-negative *S. aureus*, and their multidrug-resistant bacterial derivative strains.

Nevertheless, the irregular geometry and dynamic microenvironment of wound surfaces pose challenges for stable sensor attachment and consistent spectral acquisition. Additionally, the composition of wound exudate varies across healing stages, which can affect target molecule availability and complicate result interpretation.

Conclusion and outlook

SERS has been applied to detect various body fluids, including sweat, ISF, and wound exudate. Table 1 summarizes recent studies on SERS-based analysis of these biofluids, including plasmonic materials, substrate materials, sampling, analytes, and LOD. SERS is a promising tool in fields such as point-of-care diagnostics, remote medicine, and personalized health-

care.¹¹² At present, most SERS-integrated epidermal sensors remain at the research or prototype stage. Critical challenges remain, including substrate durability, scalable and stable nanomaterial fabrication, reliable multi-functional integration, and standardized AI validation. Overcoming these barriers will advance the development of SERS and pave the way for its clinical translation and commercialization. Future research directions can therefore be outlined in the following key areas (Figure 6).

Substrate design

Substrate design is critical for ensuring user comfort and compliance and for optimizing sampling efficiency. Common flexible polymers, such as PDMS and PU, exhibit flexibility, biocompatibility, and manufacturability. However, their limited hydration capacity, hydrophobic surfaces, and high mechanical modulus pose challenges for achieving sustained skin conformity. The

Table 1. Representative works of SERS-integrated wearable epidermal sensors

Plasmonic materials	Substrate materials	Sampling methods	Analytes	LOD	Reference
SERS-integrated sweat sensor					
AgNPs	Whatman 1 standard filter paper	paper-based microfluidics	uric acid	1.00×10^{-5} M	Li et al. ⁴³
AgNPs	glass	direct contact	uric acid	1.70×10^{-6} M	Lu et al. ⁵³
AgNWs	silk fibroin	direct contact	MB/2-FMA	1.00×10^{-8} / 2.79×10^{-4} M	Koh et al. ¹²¹
Au nanomesh	PVA	direct contact	urea/ascorbic acid	1.00×10^{-3} / 1.00×10^{-8} M	Liu et al. ⁴⁴
Ag nanomushroom	Kapton tape	microfluidics channel	lactate/urea	1.00×10^{-5} / 1.00×10^{-4} M	He et al. ⁴⁰
Au nanosphere cone	PDMS	microfluidics channel	acetaminophen	1.30×10^{-7} M	Xiao et al. ⁴⁸
AgNPs-CdSNWs/nanofilm	N/A	direct contact	urea	2.00×10^{-5} M	Luo et al. ⁶³
AAO-Au	silk fibroin membrane	direct contact	glucose	1.68×10^{-7} M	Wang et al. ⁵¹
AuNRs@DTNB@Au@MPBA	the thread-embroidered/fabric band	direct contact	lactic acid/glucose	5.00×10^{-5} / 1.25×10^{-7} M	Zhao et al. ¹²²
S-CNF-AgNPs/PAA	hydrogel	direct contact	urea/uric acid	6.31×10^{-5} / 3.98×10^{-6} M	Wang et al. ¹²³
AuNPs	Thermoplastic polyurethane (TPU)	direct contact	pH	N/A	Chung et al. ⁵²
NaNbO ₃ nanoflakes/TiO ₂ NPs	PVA	direct contact	ascorbic acid/glucose/uric acid/urea	5×10^{-7} / 8×10^{-7} / 1×10^{-6} / 1×10^{-4} M	Durai et al. ⁵⁶
PTFE/AgNWs	biocompatible and adhesive tape	microfluidics channel	lactate/urea	1.90×10^{-2} / 5.00×10^{-2} M	Foti et al. ⁴⁹
Active-site maximization of TiVC MXene	medical clear double-sided tape	direct contact	nicotine	1.00×10^{-8} M	Liu et al. ⁶¹
Ga@AgNPs	polyethylenimine ethoxylated (PEIE)-PDMS	microfluidics channel	glucose	6.17×10^{-9} M	Yuan et al. ⁴⁷
SERS-integrated ISF sensor					
AuNPs	polylactic acid	Direct contact	dyes and adenine	below 200 ppb	Chia et al. ⁸¹
AuNPs	PEGDA	3D printed hollow MN	biotin	$\sim 3.50 \times 10^{-7}$ M	Miranda et al. ⁶⁸
AuNPs	Si	3D printed hollow MN with sucker	uric acid	5.1×10^{-7} M	Xiao et al. ³²
AuNPs	carbohydrate (maltose)	Direct contact	cystatin C	7.5×10^{-9} M	Puttaswamy et al. ⁹³
Ag films	AdminPatch 1200 microneedle	Direct contact	glucose	between 5 and 150×10^{-6} M	Yuen and Liu ⁸²
4-MBA/AuNRs	Norland optical adhesive	Direct contact	pH	pH: 2–12	Park et al. ⁷⁰
Core-satellite AuNPs	PMMA	Direct contact	pyocyanin	3×10^{-5} M	Mei et al. ¹²⁴
Au nanopopcorns	TMA/CAA/HEMA/TEGDMA	Direct contact	<i>E. coli</i>	143 CFU/g	Wang et al. ⁷¹

(Continued on next page)

Table 1. Continued

Plasmonic materials	Substrate materials	Sampling methods	Analytes	LOD	Reference
Core-satellite AuNPs	PMMA	Direct contact	H ₂ O ₂	1 × 10 ⁻⁶ M	Mei et al. ⁹⁴
SERS-integrated wound sensor					
AuNPs	Band-aids	Plasmonic patch	H ₂ O ₂	6 × 10 ⁻⁷ M	Qu et al. ¹⁰⁹
AgNPs	hydrogel	Plasmonic patch	<i>S. aureus</i>	10 CFU/mL	Guo et al. ¹¹¹
AgNPs	swab	Extraction	pyocyanin	1.1 × 10 ⁻⁶ M	Tanaka et al. ¹⁰⁰
Au@SiO ₂	chitosan membrane	Plasmonic Patch	glucose	N/A	Sun et al. ⁹⁹
Au-Ag core-shell NPs	N/A	Direct analysis	ONOO ⁻	1.2 × 10 ⁻⁷ M	Chen et al. ¹⁰²
Ag nano-island	cellulose fiber	Plasmonic patch	MMP-9/TNF- α	10–500/5–25 ng/mL	Perumal et al. ¹⁰⁴
Au-AgNSs	sodium hyaluronate gel	Plasmonic patch	extended spectrum beta-Lactamase (ESBL) <i>E. coli</i> /MRSAmethicillin-resistant staphylococcus aureus (MRSA)	600/300 CFU/mL	He et al. ¹⁰¹

integration of high-elastic polymer materials (e.g., strong and tough hydrogels) into the substrate may enhance the sensor's performance under mechanical stress and extend its lifespan.¹¹³ The development of self-healing polymeric substrates (e.g., organogel composites) with low stiffness and high stretchability offers a promising route to restore sensing performance after physical damage.¹¹⁴ These materials can help mitigate performance degradation caused by repeated bending, stretching, or long-term use in dynamic environments.

Plasmonic material selection

Advancements in nanomaterial design and multi-layered plasmonic structures can improve the sensitivity and anti-interference capabilities of sensors and enhance detection efficiency. Noble metals such as Au and Ag, particularly in nanostructures (e.g., nanorods and nanostars), are preferred due to their strong and tunable LSPR. 2D materials (e.g., graphene and transition metal dichalcogenides) can also be used as plasmonic auxiliary materials due to their electronic and optical properties.¹¹⁵ For specific biomarkers with inherently weak Raman scattering cross-sections (e.g., proteins), the rational design of SERS probes is essential for achieving molecular recognition and signal enhancement, involving surface chemical modifications with selective binding capabilities, as well as the incorporation of biorecognition elements (e.g., antibodies and aptamers).¹¹⁶ It is important to consider the dynamic physiological environment, including humidity fluctuation, mechanical deformation, and temperature variations. The chemical stability and the structural integrity can prevent oxidation or structural degradation, ensuring long-term functionality.

Multi-functional integration

The combination of SERS with other spectroscopic techniques, such as laser-induced breakdown spectroscopy (LIBS; for elemental analysis),¹¹⁷ can enable simultaneous detection of molecular and atomic analytes for improving data abundance. Flexible printed circuit boards (FPCBs) integrated onto the SERS substrate can incorporate different sensors to enable

synchronized acquisition of physical and chemical information (temperature, pressure, and pH), providing comprehensive health status profiling through multi-modal data correlation.¹¹⁸ The miniaturization of SERS, through minimal optical components and wireless systems, can transform lab-grade detection into wearable devices. By integrating compact sensors with flexible designs, current limitations in device size and rigidity can be addressed.¹¹⁹

AI-driven diagnostics

The variability of target molecules between individuals and the complex biofluid composition can complicate the analysis of SERS. By applying AI algorithms to the acquired SERS fingerprint signals from biofluids, it is possible to extract biomarker features for early disease diagnostics and personalized health management.¹²⁰ AI algorithms have been applied to baseline correction, feature extraction, and classification, helping to mitigate spectral background, spectral overlap, and inter-individual variability. Such processing improves biomarker identification of SERS diagnostics. For example, integrating wearable SERS sweat sensors with multiple AI algorithms (e.g., principal-component analysis [PCA], random forest [RF], and support vector machine [SVM]) can classify lung cancer treatment responses with 89.7% accuracy while identifying potential biomarkers related to comorbidities.⁴⁶ These data-driven approaches improve diagnostic precision, enhance interpretability, and support scalable deployment of SERS-integrated epidermal sensors.

In addition to the research directions discussed above, the clinical translation of this technique requires addressing several critical challenges. For example, various materials, including precious metal materials and 2D materials, have been used to enhance Raman signals, whose long-term biocompatibility and potential toxicity remain unclear. Future studies should focus on safety assessments and the development of low-toxicity or biodegradable alternatives for continuous skin-contact use. In addition, under dynamic environments, mechanical deformation and movement

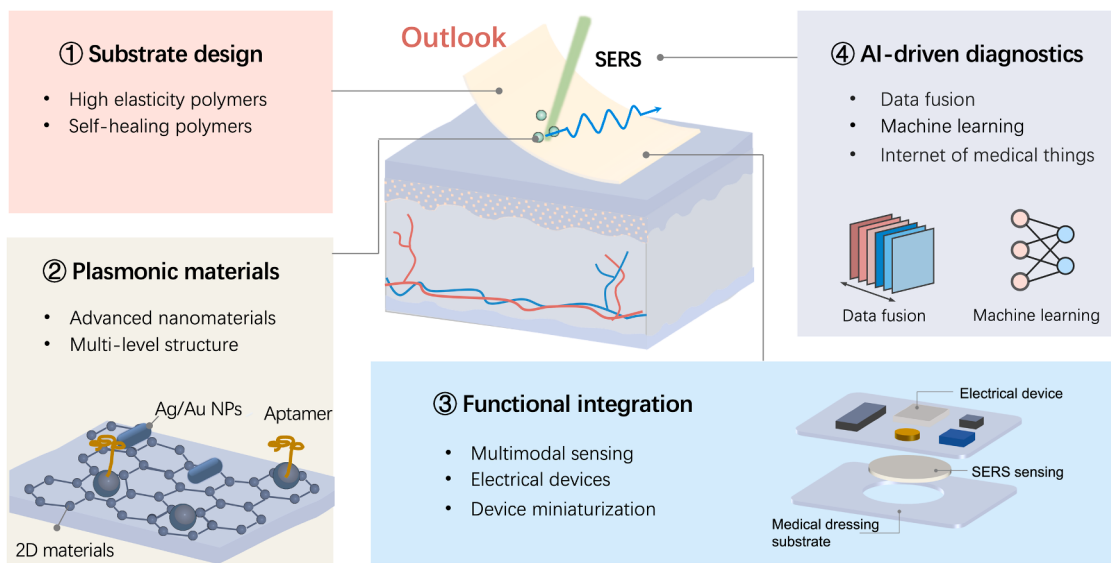


Figure 6. Outlook of SERS-integrated epidermal sensors

can change the structure of plasmonic hotspots, leading to signal fluctuations and reduced reproducibility. It is important to design mechanically stable substrates and apply signal correction methods to maintain reliable performance. The development of SERS-integrated wearable epidermal sensors requires interdisciplinary collaboration and innovation, focusing on improvements in structural design, plasmonic materials optimization, functional integration, and AI-driven diagnostics.

ACKNOWLEDGMENTS

This research was financially supported by Guangdong Province Science and Technology Plan Project 2023B1212120008, the Hong Kong Innovation and Technology Commission via the Hong Kong Branch of National Precious Metals Material Engineering Research Center, the Research Grants Council of Hong Kong through an ANR-RGC JRS grant (A-CityU101/20), the National Natural Science Foundation of China (grant no. 62475128), and the Youth Innovation Team Program of Shandong Higher Education Institution (2024KJN016).

AUTHOR CONTRIBUTIONS

Conceptualization, Y.Liu; visualization, Y.Liu, C.L., and Y.S.; investigation, Y.Liu, B.Z., X.H., Y.Long, A.C., and X.L.; methodology, Y.Liu, B.Z., S.L., C.S., and D.L.; data curation, Y.Liu, T.X., and C.L.; formal analysis, C.L. and W.L.; funding acquisition, B.Z., X.L., D.L., L.G., and C.L.; writing – original draft, Y.Liu, B.Z., and X.H.; writing – review & editing, Y.S., L.G., C.L., W.L., and C.L.

DECLARATION OF INTERESTS

All authors declare that they have no competing interests.

REFERENCES

- Brasier, N., Wang, J., Gao, W., Sempionatto, J.R., Dincer, C., Ates, H.C., Güder, F., Olenik, S., Schauwecker, I., Schaffarczyk, D., et al. (2024). Applied body-fluid analysis by wearable devices. *Nature* 636, 57–68. <https://doi.org/10.1038/s41586-024-08249-4>.
- Bariya, M., Nyein, H.Y.Y., and Javey, A. (2018). Wearable sweat sensors. *Nat. Electron.* 1, 160–171. <https://doi.org/10.1038/s41928-018-0043-y>.
- He, W., Wang, C., Wang, H., Jian, M., Lu, W., Liang, X., Zhang, X., Yang, F., and Zhang, Y. (2019). Integrated textile sensor patch for real-time and multiplex sweat analysis. *Sci. Adv.* 5, eaax0649. <https://doi.org/10.1126/sciadv.aax0649>.
- Gao, W., Emaminejad, S., Nyein, H.Y.Y., Challal, S., Chen, K., Peck, A., Fahad, H.M., Ota, H., Shiraki, H., Kiriyama, D., et al. (2016). Fully integrated wearable sensor arrays for multiplexed *in situ* perspiration analysis. *Nature* 529, 509–514. <https://doi.org/10.1038/nature16521>.
- Pu, Z., Zhang, X., Yu, H., Tu, J., Chen, H., Liu, Y., Su, X., Wang, R., Zhang, L., and Li, D. (2021). A thermal activated and differential self-calibrated flexible epidermal biomicrofluidic device for wearable accurate blood glucose monitoring. *Sci. Adv.* 7, eabd0199. <https://doi.org/10.1126/sciadv.abd0199>.
- Tehrani, F., Teymourian, H., Wuerstle, B., Kavner, J., Patel, R., Furmidge, A., Aghavali, R., Hosseini-Toudeshki, H., Brown, C., Zhang, F., et al. (2022). An integrated wearable microneedle array for the continuous monitoring of multiple biomarkers in interstitial fluid. *Nat. Biomed. Eng.* 6, 1214–1224. <https://doi.org/10.1038/s41551-022-00887-1>.
- Ge, Z., Guo, W., Tao, Y., Sun, H., Meng, X., Cao, L., Zhang, S., Liu, W., Akhtar, M.L., Li, Y., and Ren, Y. (2023). Wireless and Closed-Loop Smart Dressing for Exudate Management and On-Demand Treatment of Chronic Wounds. *Adv. Mater.* 35, e2304005. <https://doi.org/10.1002/adma.202304005>.
- Yang, Y., and Gao, W. (2019). Wearable and flexible electronics for continuous molecular monitoring. *Chem. Soc. Rev.* 48, 1465–1491. <https://doi.org/10.1039/c7cs00730b>.
- Wang, M., Yang, Y., Min, J., Song, Y., Tu, J., Mukasa, D., Ye, C., Xu, C., Hefflin, N., McCune, J.S., et al. (2022). A wearable electrochemical biosensor for the monitoring of metabolites and nutrients. *Nat. Biomed. Eng.* 6, 1225–1235. <https://doi.org/10.1038/s41551-022-00916-z>.
- Baker, L.B., Model, J.B., Barnes, K.A., Anderson, M.L., Lee, S.P., Lee, K.A., Brown, S.D., Reimel, A.J., Roberts, T.J., Nuccio, R.P., et al. (2020). Skin-interfaced microfluidic system with personalized sweating rate and sweat chloride analytics for sports science applications. *Sci. Adv.* 6, eabe3929. <https://doi.org/10.1126/sciadv.abe3929>.

11. Xiong, Z., Achavananthadith, S., Lian, S., Madden, L.E., Ong, Z.X., Chua, W., Kalidasan, V., Li, Z., Liu, Z., Singh, P., et al. (2021). A wireless and battery-free wound infection sensor based on DNA hydrogel. *Sci. Adv.* 7, eabj1617. <https://doi.org/10.1126/sciadv.abj1617>.
12. Yang, Y., Song, Y., Bo, X., Min, J., Pak, O.S., Zhu, L., Wang, M., Tu, J., Kogan, A., Zhang, H., et al. (2020). A laser-engraved wearable sensor for sensitive detection of uric acid and tyrosine in sweat. *Nat. Biotechnol.* 38, 217–224. <https://doi.org/10.1038/s41587-019-0321-x>.
13. Koh, A., Kang, D., Xue, Y., Lee, S., Pielak, R.M., Kim, J., Hwang, T., Min, S., Banks, A., Bastien, P., et al. (2016). A soft, wearable microfluidic device for the capture, storage, and colorimetric sensing of sweat. *Sci. Transl. Med.* 8, 366ra165. <https://doi.org/10.1126/scitranslmed.aaf2593>.
14. Childs, A., Mayol, B., Lasalde-Ramírez, J.A., Song, Y., Sempionatto, J.R., and Gao, W. (2024). Diving into Sweat: Advances, Challenges, and Future Directions in Wearable Sweat Sensing. *ACS Nano* 18, 24605–24616. <https://doi.org/10.1021/acsnano.4c10344>.
15. Li, Z., Wang, Y., Zhang, R., Liu, Z., Chang, Z., Deng, Y., and Qi, X. (2024). Microneedles-Based Theranostic Platform: From the Past to the Future. *ACS Nano* 18, 23876–23893. <https://doi.org/10.1021/acsnano.4c04277>.
16. Vora, L.K., Sabri, A.H., McKenna, P.E., Himawan, A., Hutton, A.R.J., Detamornrat, U., Paredes, A.J., Larrañeta, E., and Donnelly, R.F. (2023). Microneedle-based biosensing. *Nat. Rev. Bioeng.* 2, 64–81. <https://doi.org/10.1038/s44222-023-00108-7>.
17. Wang, C., Shirzaei Sani, E., Shih, C.D., Lim, C.T., Wang, J., Armstrong, D.G., and Gao, W. (2024). Wound management materials and technologies from bench to bedside and beyond. *Nat. Rev. Mater.* 9, 550–566. <https://doi.org/10.1038/s41578-024-00693-y>.
18. Chen, S., Qiao, Z., Niu, Y., Yeo, J.C., Liu, Y., Qi, J., Fan, S., Liu, X., Lee, J.Y., and Lim, C.T. (2023). Wearable flexible microfluidic sensing technologies. *Nat. Rev. Bioeng.* 1, 950–971. <https://doi.org/10.1038/s44222-023-00094-w>.
19. Song, R., Cho, S., Khan, S., Park, I., and Gao, W. (2025). Lighting the Path to Precision Healthcare: Advances and Applications of Wearable Photonic Sensors. *Adv. Mater.* 26, e2419161. <https://doi.org/10.1002/adma.202419161>.
20. Cialla-May, D., Bonifacio, A., Bocklitz, T., Markin, A., Markina, N., Fornasarò, S., Dwivedi, A., Dib, T., Farnesi, E., Liu, C., et al. (2024). Biomedical SERS - the current state and future trends. *Chem. Soc. Rev.* 53, 8957–8979. <https://doi.org/10.1039/d4cs00090k>.
21. Lee, S., Dang, H., Moon, J.I., Kim, K., Joung, Y., Park, S., Yu, Q., Chen, J., Lu, M., Chen, L., et al. (2024). SERS-based microdevices for use as *in vitro* diagnostic biosensors. *Chem. Soc. Rev.* 53, 5394–5427. <https://doi.org/10.1039/d3cs01055d>.
22. Zong, C., Xu, M., Xu, L.J., Wei, T., Ma, X., Zheng, X.S., Hu, R., and Ren, B. (2018). Surface-Enhanced Raman Spectroscopy for Bioanalysis: Reliability and Challenges. *Chem. Rev.* 118, 4946–4980. <https://doi.org/10.1021/acs.chemrev.7b00668>.
23. Lao, Z., Zheng, Y., Dai, Y., Hu, Y., Ni, J., Ji, S., Cai, Z., Smith, Z.J., Li, J., Zhang, L., et al. (2020). Nanogap Plasmonic Structures Fabricated by Switchable Capillary-Force Driven Self-Assembly for Localized Sensing of Anticancer Medicines with Microfluidic SERS. *Adv. Funct. Mater.* 30, 1909467. <https://doi.org/10.1002/adfm.201909467>.
24. Li, J.F., Zhang, Y.J., Ding, S.Y., Panneerselvam, R., and Tian, Z.Q. (2017). Core-Shell Nanoparticle-Enhanced Raman Spectroscopy. *Chem. Rev.* 117, 5002–5069. <https://doi.org/10.1021/acs.chemrev.6b00596>.
25. Boerigter, C., Campana, R., Morabito, M., and Linic, S. (2016). Evidence and implications of direct charge excitation as the dominant mechanism in plasmon-mediated photocatalysis. *Nat. Commun.* 7, 10545. <https://doi.org/10.1038/ncomms10545>.
26. Gu, Y., Li, Y., Qiu, H., Yang, Y., Wu, Q., Fan, X., Ding, Y., Yi, L., Ge, K., and Shen, Y. (2023). Recent progress on noble-free substrates for surface-enhanced Raman spectroscopy analysis. *Coord. Chem. Rev.* 497, 215425. <https://doi.org/10.1016/j.ccr.2023.215425>.
27. Cong, S., Liu, X., Jiang, Y., Zhang, W., and Zhao, Z. (2020). Surface Enhanced Raman Scattering Revealed by Interfacial Charge-Transfer Transitions. *Innovation* 1, 100051. <https://doi.org/10.1016/j.xinn.2020.100051>.
28. Ding, S.Y., You, E.M., Tian, Z.Q., and Moskovits, M. (2017). Electromagnetic theories of surface-enhanced Raman spectroscopy. *Chem. Soc. Rev.* 46, 4042–4076. <https://doi.org/10.1039/c7cs00238f>.
29. Ward, D.R., Grady, N.K., Levin, C.S., Halas, N.J., Wu, Y., Nordlander, P., and Natelson, D. (2007). Electromigrated nanoscale gaps for surface-enhanced Raman spectroscopy. *Nano Lett.* 7, 1396–1400. <https://doi.org/10.1021/nl070625w>.
30. Chen, J.Z., Liu, G., Zhu, Y.Z., Su, M., Yin, P., Wu, X.J., Lu, Q., Tan, C., Zhao, M., Liu, Z., et al. (2020). Ag@MoS₂ Core-Shell Heterostructure as SERS Platform to Reveal the Hydrogen Evolution Active Sites of Single-Layer MoS₂. *J. Am. Chem. Soc.* 142, 7161–7167. <https://doi.org/10.1021/jacs.0c01649>.
31. Han, X.X., Rodriguez, R.S., Haynes, C.L., Ozaki, Y., and Zhao, B. (2022). Surface-enhanced Raman spectroscopy. *Nat. Rev. Methods Primers* 1, 87. <https://doi.org/10.1038/s43586-021-00083-6>.
32. Xiao, J., Zhang, S., Liu, Q., Xu, T., and Zhang, X. (2024). Microfluidic-based plasmonic microneedle biosensor for uric acid ultrasensitive monitoring. *Sensor. Actuator. B Chem.* 398, 134685. <https://doi.org/10.1016/j.snb.2023.134685>.
33. Xu, K., Zhou, R., Takei, K., and Hong, M. (2019). Toward Flexible Surface-Enhanced Raman Scattering (SERS) Sensors for Point-of-Care Diagnostics. *Adv. Sci.* 6, 1900925. <https://doi.org/10.1002/advs.201900925>.
34. Wang, K., Li, Z., Li, J., and Lin, H. (2021). Raman spectroscopic techniques for nondestructive analysis of agri-foods: A state-of-the-art review. *Trends Food Sci. Technol.* 118, 490–504. <https://doi.org/10.1016/j.tifs.2021.10.010>.
35. Wang, Y., Zhao, C., Wang, J., Luo, X., Xie, L., Zhan, S., Kim, J., Wang, X., Liu, X., and Ying, Y. (2021). Wearable plasmonic-metasurface sensor for noninvasive and universal molecular fingerprint detection on bio-interfaces. *Sci. Adv.* 7, eabe4553.
36. Guo, J., Zhong, Z., Li, Y., Liu, Y., Wang, R., and Ju, H. (2019). Three-in-One" SERS Adhesive Tape for Rapid Sampling, Release, and Detection of Wound Infectious Pathogens. *ACS Appl. Mater. Interfaces* 11, 36399–36408. <https://doi.org/10.1021/acsami.9b12823>.
37. Plou, J., Valera, P.S., García, I., de Albuquerque, C.D.L., Carracedo, A., and Liz-Marzán, L.M. (2022). Prospects of Surface-Enhanced Raman Spectroscopy for Biomarker Monitoring toward Precision Medicine. *ACS Photonics* 9, 333–350. <https://doi.org/10.1021/acspophotonics.1c01934>.
38. Chen, S., Qi, J., Fan, S., Qiao, Z., Yeo, J.C., and Lim, C.T. (2021). Flexible Wearable Sensors for Cardiovascular Health Monitoring. *Adv. Healthc. Mater.* 10, e2100116. <https://doi.org/10.1002/adhm.202100116>.
39. Xie, L., Zeng, H., Zhu, J., Zhang, Z., Sun, H.b., Xia, W., and Du, Y. (2022). State of the art in flexible SERS sensors toward label-free and onsite detection: from design to applications. *Nano Res.* 15, 4374–4394. <https://doi.org/10.1007/s12274-021-4017-4>.
40. He, X., Fan, C., Luo, Y., Xu, T., and Zhang, X. (2022). Flexible microfluidic nanoplasmonic sensors for refreshable and portable recognition of sweat biochemical fingerprint. *npj Flex. Electron.* 6, 60. <https://doi.org/10.1038/s41528-022-00192-6>.
41. Mogera, U., Guo, H., Namkoong, M., Rahman, M.S., Nguyen, T., and Tian, L. (2022). Wearable plasmonic paper-based microfluidics for continuous sweat analysis. *Sci. Adv.* 8, eabn1736.
42. Han, Y., Fang, X., Li, H., Zha, L., Guo, J., and Zhang, X. (2023). Sweat Sensor Based on Wearable Janus Textiles for Sweat Collection and Microstructured Optical Fiber for Surface-Enhanced Raman Scattering Analysis. *ACS Sens.* 8, 4774–4781. <https://doi.org/10.1021/acssensors.3c01863>.

43. Li, Y., Guo, Y., Chen, H., Xiao, X., Long, F., Zhong, H., Wang, K., Guo, Z., Zhuang, Z., and Liu, Z. (2024). Flexible Wearable Plasmonic Paper-Based Microfluidics with Expandable Channel and Adjustable Flow Rate for Portable Surface-Enhanced Raman Scattering Sweat Sensing. *ACS Photonics* 11, 613–625. <https://doi.org/10.1021/acspophotonics.3c01490>.
44. Liu, L., Martinez Pancorbo, P., Xiao, T., Noguchi, S., Marumi, M., Segawa, H., Karhadkar, S., Gala de Pablo, J., Hiramatsu, K., Kitahama, Y., et al. (2022). Highly Scalable, Wearable Surface-Enhanced Raman Spectroscopy. *Adv. Opt. Mater.* 10, 2200054. <https://doi.org/10.1002/adom.202200054>.
45. Guan, P.C., Qi, Q.J., Wang, Y.Q., Lin, J.S., Zhang, Y.J., and Li, J.F. (2024). Development of a 3D Hydrogel SERS Chip for Noninvasive, Real-Time pH and Glucose Monitoring in Sweat. *ACS Appl. Mater. Interfaces* 16, 48139–48146. <https://doi.org/10.1021/acsmami.4c10817>.
46. Chen, Z., Liu, S., Yu, W., Wang, L., Lv, F., Yang, L., Yu, H., Shi, H., and Huang, Y. (2025). Hydrogel based flexible wearable sweat sensor for SERS-AI monitoring treatment effect of lung cancer. *Sensors and Actuators B-Chemical* 427, 137155. <https://doi.org/10.1016/j.snb.2024.137155>.
47. Yuan, Q., Fang, H., Wu, X., Wu, J., Luo, X., Peng, R., Xu, S., and Yan, S. (2024). Self-Adhesive, Biocompatible, Wearable Microfluidics with Erasable Liquid Metal Plasmonic Hotspots for Glucose Detection in Sweat. *ACS Appl. Mater. Interfaces* 16, 66810–66818. <https://doi.org/10.1021/acsmami.3c11746>.
48. Xiao, J., Wang, J., Luo, Y., Xu, T., and Zhang, X. (2023). Wearable Plasmonic Sweat Biosensor for Acetaminophen Drug Monitoring. *ACS Sens.* 8, 1766–1773. <https://doi.org/10.1021/acssensors.3c00063>.
49. Foti, A. (2024). Development of a wearable surface enhanced Raman scattering sensor chip based on silver nanowires for rapid detection of urea, lactate and pH in sweat. *Journal of the European Optical Society-Rapid Publications* 20, 10. <https://doi.org/10.1051/jeos/2024013>.
50. Hu, M., Zhu, K., Wei, J., Xu, Z., Yang, K., Wu, L., Zong, S., and Wang, Z. (2025). Wearable microfluidic SERS patch based on silk fibroin for the non-invasive monitoring of sweat cortisol and pH. *Sensors and Actuators B-Chemical* 427, 137152. <https://doi.org/10.1016/j.snb.2024.137152>.
51. Wang, D., Xu, G., Zhang, X., Gong, H., Jiang, L., Sun, G., Li, Y., Liu, G., Li, Y., Yang, S., and Liang, X. (2022). Dual-functional ultrathin wearable 3D particle-in-cavity SF-AAO-Au SERS sensors for effective sweat glucose and lab-on-glove pesticide detection. *Sensor. Actuator. B Chem.* 359, 131512. <https://doi.org/10.1016/j.snb.2022.131512>.
52. Chung, M., Skinner, W.H., Robert, C., Campbell, C.J., Rossi, R.M., Koutsos, V., and Radacs, N. (2021). Fabrication of a Wearable Flexible Sweat pH Sensor Based on SERS-Active Au/TPU Electrospun Nanofibers. *ACS Appl. Mater. Interfaces* 13, 51504–51518. <https://doi.org/10.1021/acsmami.1c15238>.
53. Lu, D., Cai, R., Liao, Y., You, R., and Lu, Y. (2023). Two-dimensional glass/p-ATP/Ag NPs as multifunctional SERS substrates for label-free quantification of uric acid in sweat. *Spectrochim. Acta Mol. Biomol. Spectrosc.* 296, 122631. <https://doi.org/10.1016/j.saa.2023.122631>.
54. Zhu, K., Yang, K., Zhang, Y., Yang, Z., Qian, Z., Li, N., Li, L., Jiang, G., Wang, T., Zong, S., et al. (2022). Wearable SERS Sensor Based on Omnidirectional Plasmonic Nanovoids Array with Ultra-High Sensitivity and Stability. *Small* 18, e2201508. <https://doi.org/10.1002/smll.202201508>.
55. Li, G., Zhao, X., Tang, X., Yao, L., Li, W., Wang, J., Liu, X., Han, B., Fan, X., Qiu, T., and Hao, Q. (2024). Wearable Hydrogel SERS Chip Utilizing Plasmonic Trimers for Uric Acid Analysis in Sweat. *Nano Lett.* 24, 13447–13454. <https://doi.org/10.1021/acs.nanolett.4c04267>.
56. Durai, L., and Badhulika, S. (2022). A Wearable PVA Film Supported TiO₂ Nanoparticles Decorated NaNbO₃ Nanoflakes-Based SERS Sensor for Simultaneous Detection of Metabolites and Biomolecules in Human Sweat Samples. *Adv. Mater. Interfaces* 9, 2200146. <https://doi.org/10.1002/admi.202200146>.
57. Zhang, H., Zhang, H., Sikdar, D., Liu, X., Yang, Z., Cheng, W., and Chen, Y. (2024). Jellyfish-like Gold Nanowires as FlexoSERS Sensors for Sweat Analysis. *Nano Lett.* 24, 11269–11278. <https://doi.org/10.1021/acs.nanolett.4c02907>.
58. Chen, Z., Liu, Y., Yu, W., Liu, S., and Huang, Y. (2025). Machine Learning-Driven Wearable Sweat Sensors with AgNW/MXene for Non-Invasive SERS-Based Cardiovascular Disease Detection. *ACS Appl. Nano Mater.* 8, 5602–5610. <https://doi.org/10.1021/acsnano.4c07355>.
59. Yu, W., Li, Q., Ren, J., Feng, K., Gong, J., Li, Z., Zhang, J., Liu, X., Xu, Z., and Yang, L. (2024). A sensor platform based on SERS detection/janus textile for sweat glucose and lactate analysis toward portable monitoring of wellness status. *Biosens. Bioelectron.* 263, 116612. <https://doi.org/10.1016/j.bios.2024.116612>.
60. Liang, X., Li, N., Zhang, R., Yin, P., Zhang, C., Yang, N., Liang, K., and Kong, B. (2021). Carbon-based SERS biosensor: from substrate design to sensing and bioapplication. *NPG Asia Mater.* 13, 8. <https://doi.org/10.1038/s41427-020-00278-5>.
61. Liu, X., Li, T., Lee, T.C., Sun, Y., Liu, Y., Shang, L., Han, Y., Deng, W., Yuan, Z., and Dang, A. (2024). Wearable Plasmonic Sensors Engineered via Active-Site Maximization of TiC MXene for Universal Physiological Monitoring at the Molecular Level. *ACS Sens.* 9, 483–493. <https://doi.org/10.1021/acssensors.3c02285>.
62. Xiong, S., Wang, C., Zhu, C., Dong, P., and Wu, X. (2024). Dual Detection of Urea and Glucose in Sweat Using a Portable Microfluidic SERS Sensor with Silver Nano-Triponds and 1D-CNN Model Analysis. *ACS Appl. Mater. Interfaces* 16, 65918–65926. <https://doi.org/10.1021/acsmami.4c14962>.
63. Luo, Y., Zhai, B., Li, M., Zhou, W., Yang, J., Shu, Y., and Fang, Y. (2024). Self-adhesive, surface adaptive, regenerable SERS substrates for in-situ detection of urea on bio-surfaces. *J. Colloid Interface Sci.* 660, 513–521. <https://doi.org/10.1016/j.jcis.2024.01.068>.
64. Kesava Rao, V., Tang, X., Sekine, Y., Egawa, M., Dwivedi, P.K., Kitahama, Y., Yang, W., and Goda, K. (2023). An Ultralow-Cost, Durable, Flexible Substrate for Ultrabroadband Surface-Enhanced Raman Spectroscopy. *Advanced Photonics Research* 5, 2300291. <https://doi.org/10.1002/adpr.202300291>.
65. Wu, Z., Qiao, Z., Chen, S., Fan, S., Liu, Y., Qi, J., and Lim, C.T. (2024). Interstitial fluid-based wearable biosensors for minimally invasive healthcare and biomedical applications. *Commun. Mater.* 5, 33. <https://doi.org/10.1038/s43246-024-00468-6>.
66. Kim, G., Ahn, H., Chaj Ulloa, J., and Gao, W. (2024). Microneedle sensors for dermal interstitial fluid analysis. *Med. X.* 2, 15.
67. Hsieh, Y.C., Lin, C.Y., Lin, H.Y., Kuo, C.T., Yin, S.Y., Hsu, Y.H., Yeh, H.F., Wang, J., and Wan, D. (2023). Controllable-Swelling Microneedle-Assisted Ultrasensitive Paper Sensing Platforms for Personal Health Monitoring. *Adv. Healthc. Mater.* 12, e2300321. <https://doi.org/10.1002/adhm.202300321>.
68. Miranda, B., Battisti, M., De Martino, S., Nocerino, V., Dardano, P., De Stefano, L., and Cangiano, G. (2023). Hollow Microneedle-based Plasmonic Sensor for on Patch Detection of Molecules in Dermal Interstitial Fluid. *Adv. Mater. Technol.* 8, 2300037. <https://doi.org/10.1002/admt.202300037>.
69. Linh, V.T.N., Yim, S.G., Mun, C., Yang, J.Y., Lee, S., Yoo, Y.W., Sung, D.K., Lee, Y.I., Kim, D.H., Park, S.G., et al. (2021). Bioinspired plasmonic nanoflower-decorated microneedle for label-free intradermal sensing. *Appl. Surf. Sci.* 551, 149411. <https://doi.org/10.1016/j.apsusc.2021.149411>.
70. Park, J.E., Yonet-Tanyeri, N., Vander Ende, E., Henry, A.I., Perez White, B.E., Mrksich, M., and Van Duyne, R.P. (2019). Plasmonic Microneedle Arrays for In Situ Sensing with Surface-Enhanced Raman Spectroscopy (SERS). *Nano Lett.* 19, 6862–6868. <https://doi.org/10.1021/acs.nanolett.9b02070>.
71. Wang, Y., Ni, H., Li, H., Chen, J., Zhang, D., and Fu, L. (2022). Plasmonic microneedle arrays for rapid extraction, SERS detection, and inactivation

- of bacteria. *Chem. Eng. J.* 442, 136140. <https://doi.org/10.1016/j.cej.2022.136140>.
72. Li, X., Zhou, S., Deng, Z., Liu, B., and Gao, B. (2024). Corn-inspired high-density plasmonic metal-organic frameworks microneedles for enhanced SERS detection of acetaminophen. *Talanta* 278, 126463. <https://doi.org/10.1016/j.talanta.2024.126463>.
73. Chen, Z., Guo, Y., Gu, X., Liu, X., Zhang, J., Song, C., and Wang, L. (2024). Flexible plasmonic microneedle array-based SERS sensor for pH monitoring of skin interstitial fluid. *Microchem. J.* 206, 111546. <https://doi.org/10.1016/j.microc.2024.111546>.
74. Li, Y., Wang, Y., Mei, R., Lv, B., Zhao, X., Bi, L., Xu, H., and Chen, L. (2024). Hydrogel-Coated SERS Microneedles for Drug Monitoring in Dermal Interstitial Fluid. *ACS Sens.* 9, 2567–2574. <https://doi.org/10.1021/acssensors.4c00276>.
75. Hu, Y., Chatzilakou, E., Pan, Z., Traverso, G., and Yetisen, A.K. (2024). Microneedle Sensors for Point-of-Care Diagnostics. *Adv. Sci.* 11, e2306560. <https://doi.org/10.1002/advs.202306560>.
76. Sang, M., Cho, M., Lim, S., Min, I.S., Han, Y., Lee, C., Shin, J., Yoon, K., Yeo, W.H., Lee, T., et al. (2023). Fluorescent-based biodegradable microneedle sensor array for tether-free continuous glucose monitoring with smartphone application. *Sci. Adv.* 9, eadh1765. <https://doi.org/10.1126/sciadv.adh1765>.
77. Kashaninejad, N., Munaz, A., Moghadas, H., Yadav, S., Umer, M., and Nguyen, N.T. (2021). Microneedle Arrays for Sampling and Sensing Skin Interstitial Fluid. *Chemosensors* 9, 83. <https://doi.org/10.3390/chemosensors9040083>.
78. Brasiliense, V., Park, J.E., Berns, E.J., Van Duyne, R.P., and Mrksich, M. (2022). Surface potential modulation as a tool for mitigating challenges in SERS-based microneedle sensors. *Sci. Rep.* 12, 15929. <https://doi.org/10.1038/s41598-022-19942-7>.
79. Lin, S., Ouyang, Y., Lin, W., Zhou, X., Miao, M., Cheng, E., Jiang, Y., Meng, Z., Jin, M., Zhang, S., et al. (2024). Microenvironment-optimized GelMA microneedles for interstitial fluid extraction and real-time glucose detection. *Surf. Interfaces* 45, 103847. <https://doi.org/10.1016/j.surfin.2024.103847>.
80. Takeuchi, K., Takama, N., Kim, B., Sharma, K., Paul, O., and Ruther, P. (2019). Microfluidic chip to interface porous microneedles for ISF collection. *Biomed. Microdevices* 21, 28. <https://doi.org/10.1007/s10544-019-0370-4>.
81. Chia, Z.C., Chen, Y.L., Chuang, C.H., Hsieh, C.H., Chen, Y.J., Chen, K.H., Huang, T.C., Chen, M.C., and Huang, C.C. (2023). Polyphenol-assisted assembly of Au-deposited poly(lactic acid) microneedles for SERS sensing and antibacterial photodynamic therapy. *Chem. Commun.* 59, 6339–6342. <https://doi.org/10.1039/d3cc00733b>.
82. Yuen, C., and Liu, Q. (2014). Towards in vivo intradermal surface enhanced Raman scattering (SERS) measurements: silver coated micro-needle based SERS probe. *J. Biophotonics* 7, 683–689. <https://doi.org/10.1002/bio.201300006>.
83. Dabbagh, S.R., Sarabi, M.R., Rahbarghazi, R., Sokullu, E., Yetisen, A.K., and Tasoglu, S. (2021). 3D-printed microneedles in biomedical applications. *iScience* 24, 102012. <https://doi.org/10.1016/j.isci.2020.102012>.
84. Rad, Z.F., Prewett, P.D., and Davies, G.J. (2021). High-resolution two-photon polymerization: the most versatile technique for the fabrication of microneedle arrays. *Microsystems & Nanoengineering* 7, 71. <https://doi.org/10.1038/s41378-021-00298-3>.
85. Dardano, P., Caliò, A., Di Palma, V., Bevilacqua, M.F., Di Matteo, A., and De Stefano, L. (2015). A Photolithographic Approach to Polymeric Microneedles Array Fabrication. *Materials* 8, 8661–8673. <https://doi.org/10.3390/ma8125484>.
86. Pillai, M.M., Ajesh, S., and Tayalia, P. (2023). Two-photon polymerization based reusable master template to fabricate polymer microneedles for drug delivery. *MethodsX* 10, 102025.
87. Reynoso, M., Chang, A.Y., Wu, Y., Murray, R., Suresh, S., Dugas, Y., Wang, J., and Arroyo-Currás, N. (2024). 3D-printed, aptamer-based microneedle sensor arrays using magnetic placement on live rats for pharmacokinetic measurements in interstitial fluid. *Biosens. Bioelectron.* 244, 115802. <https://doi.org/10.1016/j.bios.2023.115802>.
88. Huang, X., Zheng, S., Liang, B., He, M., Wu, F., Yang, J., Chen, H.J., and Xie, X. (2023). 3D-assembled microneedle ion sensor-based wearable system for the transdermal monitoring of physiological ion fluctuations. *Microsyst. Nanoeng.* 9, 25. <https://doi.org/10.1038/s41378-023-00497-0>.
89. Chen, Y.W., Chen, M.C., Wu, K.W., and Tu, T.Y. (2020). A Facile Approach for Rapid Prototyping of Microneedle Molds, Microwells and Micro-Through-Holes in Various Substrate Materials Using CO₂ Laser Drilling. *Biomedicines* 8, 427. <https://doi.org/10.3390/biomedicines8100427>.
90. Shi, S., Wang, Y., Mei, R., Zhao, X., Liu, X., and Chen, L. (2023). Revealing drug release and diffusion behavior in skin interstitial fluid by surface-enhanced Raman scattering microneedles. *J. Mater. Chem. B* 11, 3097–3105. <https://doi.org/10.1039/d2tb02600g>.
91. Yang, Y., Wang, X., Hu, Y., Liu, Z., Ma, X., Feng, F., Zheng, F., Guo, X., Liu, W., Liao, W., and Han, L. (2025). Rapid enrichment and SERS differentiation of various bacteria in skin interstitial fluid by 4-MPBA-AuNPs-functionalized hydrogel microneedles. *J. Pharm. Anal.* 15, 101152. <https://doi.org/10.1016/j.jpha.2024.101152>.
92. Chang, H., Zheng, M., Yu, X., Than, A., Seenii, R.Z., Kang, R., Tian, J., Khanh, D.P., Liu, L., Chen, P., and Xu, C. (2017). A Swellable Microneedle Patch to Rapidly Extract Skin Interstitial Fluid for Timely Metabolic Analysis. *Adv. Mater.* 29, 1702243. <https://doi.org/10.1002/adma.201702243>.
93. Puttaswamy, S.V., Lubarsky, G.V., Kelsey, C., Zhang, X., Finlay, D., McLaughlin, J.A., and Bhalla, N. (2020). Nanophotonic-Carbohydrate Lab-on-a-Microneedle for Rapid Detection of Human Cystatin C in Finger-Pryk Blood. *ACS Nano* 14, 11939–11949. <https://doi.org/10.1021/acsnano.0c05074>.
94. Mei, R., Wang, Y., Zhao, X., Shi, S., Wang, X., Zhou, N., Shen, D., Kang, Q., and Chen, L. (2023). Skin Interstitial Fluid-Based SERS Tags Labeled Microneedles for Tracking of Peritonitis Progression and Treatment Effect. *ACS Sens.* 8, 372–380. <https://doi.org/10.1021/acssensors.2c02409>.
95. Chinnamani, M.V., Hanif, A., Kannan, P.K., Kaushal, S., Sultan, M.J., and Lee, N.E. (2023). Soft microfiber-based hollow microneedle array for stretchable microfluidic biosensing patch with negative pressure-driven sampling. *Biosens. Bioelectron.* 237, 115468. <https://doi.org/10.1016/j.bios.2023.115468>.
96. Abbasiasl, T., Mirlou, F., Mirzajani, H., Bathaei, M.J., Istif, E., Shomalizadeh, N., Cebeçioğlu, R.E., Özkarahan, E.E., Yener, U.C., and Beker, L. (2024). A Wearable Touch-Activated Device Integrated with Hollow Microneedles for Continuous Sampling and Sensing of Dermal Interstitial Fluid (Adv. Mater. 2/2024). *Adv. Mater.* 36, 2470012. <https://doi.org/10.1002/adma.202470012>.
97. Takeuchi, K., Takama, N., Sharma, K., Paul, O., Ruther, P., Suga, T., and Kim, B. (2022). Microfluidic chip connected to porous microneedle array for continuous ISF sampling. *Drug Deliv. Transl. Res.* 12, 435–443. <https://doi.org/10.1007/s13346-021-01050-0>.
98. Ju, J., Hsieh, C.M., Tian, Y., Kang, J., Chia, R., Chang, H., Bai, Y., Xu, C., Wang, X., and Liu, Q. (2020). Surface Enhanced Raman Spectroscopy Based Biosensor with a Microneedle Array for Minimally Invasive In Vivo Glucose Measurements. *ACS Sens.* 5, 1777–1785. <https://doi.org/10.1021/acssensors.0c00444>.
99. Sun, J., Han, S., Wang, Y., Zhao, G., Qian, W., and Dong, J. (2018). Detection of Redox State Evolution during Wound Healing Process Based on a Redox-Sensitive Wound Dressing. *Anal. Chem.* 90, 6660–6665. <https://doi.org/10.1021/acs.analchem.8b00471>.

100. Tanaka, Y., Khoo, E.H., Salleh, N.A.B.M., Teo, S.L., Ow, S.Y., Sutarlie, L., and Su, X. (2021). A portable SERS sensor for pyocyanin detection in simulated wound fluid and through swab sampling. *Analyst* 146, 6924–6934. <https://doi.org/10.1039/d1an01360b>.
101. He, J., Qiao, Y., Zhang, H., Zhao, J., Li, W., Xie, T., Zhong, D., Wei, Q., Hua, S., Yu, Y., et al. (2020). Gold-silver nanoshells promote wound healing from drug-resistant bacteria infection and enable monitoring via surface-enhanced Raman scattering imaging. *Biomaterials* 234, 119763. <https://doi.org/10.1016/j.biomaterials.2020.119763>.
102. Chen, H., Lin, S., Zhang, D., Xing, Y., Yu, F., and Wang, R. (2023). Ratiometric SERS imaging for indication of peroxynitrite fluctuations in diabetic wound healing process. *Chem. Eng. J.* 470, 144024. <https://doi.org/10.1016/j.cej.2023.144024>.
103. Zuhayri, H., Samarinova, A.A., Borisov, A.V., Guardado, D.A.L., Baalbaki, H., Krivova, N.A., and Kistenev, Y.V. (2023). Quantitative Assessment of Low-Dose Photodynamic Therapy Effects on Diabetic Wound Healing Using Raman Spectroscopy. *Pharmaceutics* 15, 595. <https://doi.org/10.3390/pharmaceutics15020595>.
104. Perumal, J., Lim, H.Q., Attia, A.B.E., Raziq, R., Leavesley, D.I., Upton, Z., Dinish, U.S., and Olivo, M. (2021). Novel Cellulose Fibre-Based Flexible Plasmonic Membrane for Point-of-Care SERS Biomarker Detection in Chronic Wound Healing. *Int. J. Nanomedicine* 16, 5869–5878. <https://doi.org/10.2147/IJN.S303130>.
105. Zheng, Z., Xing, J., Shi, H., Wu, M., Yang, R., Yao, P., and Xu, R.X. (2022). 2D scanning SERS probe for early biofilm boundary determination. *Sensor. Actuator. B Chem.* 363, 131822. <https://doi.org/10.1016/j.snb.2022.131822>.
106. Gao, X., Wu, H., Hao, Z., Ji, X., Lin, X., Wang, S., and Liu, Y. (2020). A multifunctional plasmonic chip for bacteria capture, imaging, detection, and in situ elimination for wound therapy. *Nanoscale* 12, 6489–6497. <https://doi.org/10.1039/d0nr00638f>.
107. Liu, Z., Li, S., Yin, Z., Zhu, Z., Chen, L., Tan, W., and Chen, Z. (2022). Stabilizing Enzymes in Plasmonic Silk Film for Synergistic Therapy of In Situ SERS Identified Bacteria. *Adv. Sci.* 9, e2104576. <https://doi.org/10.1002/advs.202104576>.
108. Gao, Q., Liu, R., Wu, Y., Wang, F., and Wu, X. (2024). Versatile self-assembled near-infrared SERS nanoprobes for multidrug-resistant bacterial infection-specific surveillance and therapy. *Acta Biomater.* 189, 559–573. <https://doi.org/10.1016/j.actbio.2024.09.054>.
109. Qu, L., Han, J., Huang, Y., Yang, G., Liu, W., Long, Z., Gu, Y., Zhang, Q., Gao, M., and Dong, X. (2023). Peroxidase-like Nanozymes for Point-of-Care SERS Sensing and Wound Healing. *ACS Appl. Bio Mater.* 6, 1272–1282. <https://doi.org/10.1021/acsabm.3c00008>.
110. Chen, M., Liu, G., Wang, L., Zhang, A., Yang, Z., Li, X., Zhang, Z., Gu, S., Cui, D., Haick, H., and Tang, N. (2025). Neural Network-Enhanced Electrochemical/SERS Dual-Mode Microfluidic Platform for Accurate Detection of Interleukin-6 in Diabetic Wound Exudates. *Anal. Chem.* 97, 4397–4406. <https://doi.org/10.1021/acs.analchem.4c05537>.
111. Guo, Y., Li, Y., Fan, R., Liu, A., Chen, Y., Zhong, H., Liu, Y., Chen, H., Guo, Z., and Liu, Z. (2023). Silver@Prussian Blue Core-Satellite Nanostructures as Multimetal Ions Switch for Potent Zero-Background SERS Bioimaging-Guided Chronic Wound Healing. *Nano Lett.* 23, 8761–8769. <https://doi.org/10.1021/acs.nanolett.3c02857>.
112. Liu, G., Mu, Z., Guo, J., Shan, K., Shang, X., Yu, J., and Liang, X. (2022). Surface-enhanced Raman scattering as a potential strategy for wearable flexible sensing and point-of-care testing non-invasive medical diagnosis. *Front. Chem.* 10, 1060322. <https://doi.org/10.3389/fchem.2022.1060322>.
113. Li, X., and Gong, J.P. (2024). Design principles for strong and tough hydrogels. *Nat. Rev. Mater.* 9, 380–398. <https://doi.org/10.1038/s41578-024-00672-3>.
114. Zhao, Y., Ohm, Y., Liao, J., Luo, Y., Cheng, H.Y., Won, P., Roberts, P., Carneiro, M.R., Islam, M.F., Ahn, J.H., et al. (2023). A self-healing electrically conductive organogel composite. *Nat. Electron.* 6, 206–215. <https://doi.org/10.1038/s41928-023-00932-0>.
115. Li, Z., Zhai, L., Zhang, Q., Zhai, W., Li, P., Chen, B., Chen, C., Yao, Y., Ge, Y., Yang, H., et al. (2024). 1T'-transition metal dichalcogenide monolayers stabilized on 4H-Au nanowires for ultrasensitive SERS detection. *Nat. Mater.* 23, 1355–1362. <https://doi.org/10.1038/s41563-024-01860-w>.
116. Schuknecht, F., Kolataj, K., Steinberger, M., Liedl, T., and Lohmueller, T. (2023). Accessible hotspots for single-protein SERS in DNA-origami assembled gold nanorod dimers with tip-to-tip alignment. *Nat. Commun.* 14, 7192. <https://doi.org/10.1038/s41467-023-42943-7>.
117. Palleschi, V., Legnaioli, S., Poggialini, F., Bredice, F.O., Urbina, I.A., Lelouche, N., and Messaoud Aberkane, S. (2025). Laser-induced breakdown spectroscopy. *Nat. Rev. Methods Primers* 5, 17. <https://doi.org/10.1038/s43586-025-00388-w>.
118. Mahato, K., Saha, T., Ding, S., Sandhu, S.S., Chang, A.Y., and Wang, J. (2024). Hybrid multimodal wearable sensors for comprehensive health monitoring. *Nat. Electron.* 7, 735–750. <https://doi.org/10.1038/s41928-024-01247-4>.
119. Min, S., Geng, H., He, Y., Xu, T., Liu, Q., and Zhang, X. (2025). Minimally and non-invasive glucose monitoring: the road toward commercialization. *Sens. Diagn.* 4, 370–396. <https://doi.org/10.1039/d4sd00360h>.
120. Chen, Z., Wang, W., Tian, H., Yu, W., Niu, Y., Zheng, X., Liu, S., Wang, L., and Huang, Y. (2024). Wearable intelligent sweat platform for SERS-AI diagnosis of gout. *Lab Chip* 24, 1996–2004. <https://doi.org/10.1039/d3lc01094e>.
121. Koh, E.H., Lee, W.C., Choi, Y.J., Moon, J.I., Jang, J., Park, S.G., Choo, J., Kim, D.H., and Jung, H.S. (2021). A Wearable Surface-Enhanced Raman Scattering Sensor for Label-Free Molecular Detection. *ACS Appl. Mater. Interfaces* 13, 3024–3032. <https://doi.org/10.1021/acsami.0c18892>.
122. Zhao, Z., Li, Q., Dong, Y., Gong, J., Li, Z., and Zhang, J. (2022). Core-shell structured gold nanorods on thread-embroidered fabric-based microfluidic device for Ex Situ detection of glucose and lactate in sweat. *Sensor. Actuator. B Chem.* 353, 131154. <https://doi.org/10.1016/j.snb.2021.131154>.
123. Wang, W., Chen, Y., Xiao, C., Xiao, S., Wang, C., Nie, Q., Xu, P., Chen, J., You, R., Zhang, G., and Lu, Y. (2023). Flexible SERS wearable sensor based on nanocomposite hydrogel for detection of metabolites and pH in sweat. *Chem. Eng. J.* 474, 145953. <https://doi.org/10.1016/j.cej.2023.145953>.
124. Mei, R., Wang, Y., Shi, S., Zhao, X., Zhang, Z., Wang, X., Shen, D., Kang, Q., and Chen, L. (2022). Highly Sensitive and Reliable Internal-Standard Surface-Enhanced Raman Scattering Microneedles for Determination of Bacterial Metabolites as Infection Biomarkers in Skin Interstitial Fluid. *Anal. Chem.* 94, 16069–16078. <https://doi.org/10.1021/acs.analchem.2c03208>.